Universidade de Aveiro Departamento de Biologia

2012

Fernanda de Oliveira Esteves Rosário

Efeitos de Nanopartículas de Prata em Células de Osso e Pulmão Humano

Effects of Silver Nanoparticles on Osteosarcoma and Lung Cell Lines

Universidade de Aveiro Departamento de Biologia
2012

Fernanda de Oliveira Esteves Rosário

Efeitos de Nanopartículas de Prata em Células de Osso e Pulmão Humano

Effects of Silver Nanoparticles on Osteosarcoma and Lung Cell Lines

Dissertação apresentada à Universidade de Aveiro para cumprimento dos requisitos necessários à obtenção do grau de Mestre em Biologia Aplicada, ramo de Biologia Molecular e Celular, realizada sob a orientação científica da Dra. Helena Cristina Correia de Oliveira, Pós-Doutoranda do Departamento de Biologia da Universidade de Aveiro e sob co-orientação científica da Professora Doutora Conceição Santos do Departamento de Biologia da Universidade de Aveiro

This work was supported by COMPET program/FCT (Fundação para a Ciência e Tecnologia) with the project “ASSAY - Assessment of fate and effects of Silver nanoparticles in Aquatic ecosystems” (2011-2014) PTDC/AAC-AMB/113649/2009

Dedico este trabalho aos meus pais e irmã pelo incansável apoio, amor e paciência. E por último, mas não menos importante, ao meu namorado pelo apoio, companheirismo e segurança que me deu durante este tempo.

O júri

Presidente	Prof. Dr. João António de Almeida Serôdio Professor auxiliar do departamento de Biologia da Universidade de Aveiro
Arguente principal	José Miguel Pimenta Ferreira de Oliveira Investigador Pós-Doutoramento, CESAM - Centro de Estudos do Ambiente e do Mar, Universidade de Aveiro
Orientadora	Dra. Helena Cristina Correia de Oliveira Investigadora Pós-Doutoramento, CESAM - Centro de Estudos do Ambiente e do Mar da Universidade de Aveiro
Co-orientadora	Prof. Dra. Maria Da Conceição Lopes Vieira dos Santos Professora Associada com Agregação do Departamento de Biologia da Universidade de Aveiro

palavras-chave

Nanopartículas de prata, AgNPs revestidas, AgNPS não revestidas, A549, MG-63, toxicidade, apoptose, paragem do ciclo celular.

resumo

As nanopartículas são definidas como partículas com dimensão entre 1 - 100 nm, resultando em propriedades únicas que podem ser úteis em diversas áreas. As AgNP são as nanopartículas mais utilizadas em produtos comerciais, como: curativos, cateteres, próteses, cosméticos, têxteis e produção de alimentos, devido à sua atividade antimicrobiana. As propriedades físico-químicas únicas inerentes às NPs enfatizam a necessidade de uma avaliação adequada dos potenciais efeitos tóxicos, já que suas interacções com sistemas biológicos, bem como o seu destino ambiental são imprevisíveis. As propriedades da superfície das NPs são de importância essencial para a sua capacidade de agregação, influenciando na mobilidade e absorção celular.

Neste estudo, avaliaram-se os efeitos tóxicos de AgNPs não revestidas e revestidas, na viabilidade das linhas celulares de osteossarcoma (MG-63) e adenocarcinoma do pulmão (A549). Para isso, células cultivadas *in vitro* foram expostas a concentrações crescentes de AgNPs até 400µg/ml (não revestidas - <100nm) e até 100ug/ml (revestidas com PVP – 10 e 20nm), durante 24h e 48h. O crescimento celular e morfologia foram observados diariamente, utilizando um microscópio invertido e a viabilidade celular foi medida pelo ensaio MTT. Para AgNPs não revestidas (24h e 48h), os ensaios de MTT e Trypan Blue, revelam uma disparidade de resultados sendo, ambos inconclusivos. No entanto, para as AgNPs revestidas, os ensaios de MTT independentes, mostraram resultados consistentes e fiáveis, com uma diminuição significativa da viabilidade celular a 50µg/ml. As AgNPs também modulam a distribuição do ciclo celular através da acumulação de células em G2/M, e concomitante diminuição de células em G0/G1, juntamente com o aumento da apoptose. Em conjunto, estes resultados sugerem que AgNPs induzem toxicidade, apoptose e paragem do ciclo celular em G2, nas linhas celulares A549 e MG-63.

keywords

Silver Nanoparticles, coated AgNPs, uncoate AgNPs, A549, MG-63, toxicity, apoptosis, cell cycle arrest.

abstract

Nanoparticles are defined as particles with at least one dimension between 1 – 100nm and this small size results in unique properties that can be useful in a range of fields. Silver nanoparticles (AgNPs) are the most widely used nanoparticles in commercial products, viz wound dressings, catheters, prosthesis, cosmetics, textiles and food production, due to their antimicrobial activity. The unique physicochemical properties of NPs emphasize the need for proper assessment of the potential toxic effects, since their unpredicted interactions with biological systems and environmental fate. The surface properties of NPs are of essential importance for their aggregation behavior, and this influences their mobility in environmental partitions and cellular uptake. In this study, we evaluated the toxic effects of uncoated and coated AgNP on the viability osteosarcoma (MG-63) and lung (A549) cell lines. For this, in vitro cultured cells were exposed to different increasing concentrations of AgNPs up to 400µg/mL (uncoated - <100nm) and up to 100µg/ml (PVP coated – 10 and 20nm) for 24h and 48h. Cell growth and morphology was daily observed using an inverted microscope and cell viability was measured by MTT reduction assay. For uncoated AgNPs (24h and 48h), MTT assays and Trypan Blue and reveal a disparity of results being both inconclusive. However, for the coated AgNPs, independent MTT assays showed consistent and reliable results, with a significant decrease in cell viability at the 50µg/ml. AgNPs also modulated cell cycle distribution through the accumulation of cells at G2/M and a concurrent decrease in cells at G0/G1 along with the increase on apoptotic cells. This effect was observed in both cell lines. Together, these results suggest that AgNPs induce toxicity, apoptosis and G2 cell cycle arrest in A549 and MG-63 cells.

List of Figures

Fig. 1 - Example of MG-63 pictures after 24h of AgNPs exposure: A - Control; B - 50mg/ml; C - 200mg/ml; D - 400mg/ml. 1000X. 29
Fig. 2 - Light microscopy images of MG-63 cells exposed to AgNPs for 48h: A - Control; B - 200mg/ml; C - 400mg/ml. 400X 29
Fig. 3 - Effects of AgNPs on MG-63 cell viability evaluated by two independent Trypan Blue exclusion tests, for 24h and 48h after exposure 30
Fig. 4 - Effects of Uncoated AgNPs in MG-63 cell viability (mean ± standard deviation) for 24h and 48h exposure, evaluated by three and two independent MTT assays. 31
Fig. 5 - Light microscopy images of MG-63 cells exposed to AgNPs for 24h: A - Control; B - 50mg/ml (10nm AgNP); C - 50mg/ml (20nm AgNP). 400X 33
Fig. 6 - Light microscopy images of A549 cells exposed to AgNPs for 24h: A - Control; B - 50mg/ml (10nm AgNP); C - 50mg/ml (20nm AgNP). 400X 33
Fig. 7 - Effects of Coated AgNPs – 10nm and 20nm, in MG-63 cell viability (mean ± standard deviation) for 24h exposure, evaluated by three independent MTT assays,.. Different letters represent differences between AgNPs sizes and * represent differences between concentrations and control. 34
Fig. 8 - AgNPs effects in MG-63 cell viability (%) (mean ± standard deviation) to 48h time of exposure for the MTT Assay. * indicates differences between control and AgNP concentrations ($p < 0.05$). 34
Fig. 9 - Effects of Coated AgNPs – 10nm and 20nm, in A549 cell viability (mean ± SD) for 24h exposure, evaluated by three independent MTT assays. Different letters represent differences between AgNPs sizes within a concentration ($p < 0.05$). * indicates significant differences between AgNPs concentrations and control ($p < 0.05$). 35
Fig. 10 - AgNPs effects in A549 cell viability (mean ± standard deviation) to 48h time of exposure for the MTT Assay. Different letters within concentrations represent differences between AgNPs sizes ($p < 0.05$). *indicates significant differences between AgNPs concentrations ($p < 0.05$). 36
Fig. 12 - Cell cycle results of MG-63 AgNP exposure after 24 h. The given values are the mean % of cell population (± standard deviation) along cell cycle stages of at least 3 replicates. * indicates differences between AgNP size's within a concentration at $p < 0.05$. 38
Fig. 13 - Cell cycle results of A549 AgNP exposure after 24 h. The given values are the mean % of cell population (± standard deviation) along cell cycle stages of at least 3 replicates. *indicates differences betwee AgNP size's within a concentration at $p < 0.05$ 38
Fig. 14 - Annexin V-FITC assay for apoptosis assessment of MG-63 cell line. Results for 24h exposures to 10nm and 20nm AgNPs with 3 replicates. ± SD. 39
Fig. 15 - Annexin V-FITC assay for apoptosis assessment of MG-63 cell line. Results for 48h exposures to 10nm and 20nm AgNPs with 3 replicates. ± SD. * $p<0.05$. 39
Fig. 16 - Annexin V-FITC assay for apoptosis assessment of A549 cell line. Results for 24h exposure to 10nm and 20nm AgNPs with 3 replicates. *indicates differences between control and AgNP concentrations at $p < 0.05$. 40
Fig. 17 - Annexin V-FITC assay for apoptosis assessment of A549 cell line. Results for 48h exposure to 10nm and 20nm AgNPs with 3 replicates. * indicates differences between control and AgNP concentrations at $p < 0.05$. 40

List of Tables

TABLE 1 – DLS MEASUREMENTS OF HYDRODYNAMIC DIAMETER OF UNCOATED SILVER NANOPARTICLES, 0H AFTER SOLUTIONS PREPARATIONS (T=0) – 10, 50, 100 AND 400µG/ML. SOLUTIONS WERE PREPARED BY DILUTION WITH COMPLETE GROWTH MEDIA - A-MEM - 5% FBS. IN THE PRESENCE OF MORE THAN ONE PEAK OF SIZE DISTRIBUTION, THE PEAK OF HIGHER PERCENTAGE (AND THE RESPECTIVE PERCENTAGE) WAS SHOWN. 28

TABLE 2 - DLS MEASUREMENTS OF HYDRODYNAMIC DIAMETER OF UNCOATED SILVER NANOPARTICLES, 24H AFTER SOLUTIONS PREPARATIONS(T=24) – 10, 50, 100 AND 400µG/ML. SOLUTIONS WERE PREPARED BY DILUTION WITH COMPLETE GROWTH MEDIA - A-MEM - 5% FBS. IN THE PRESENCE OF MORE THAN ONE PEAK OF SIZE DISTRIBUTION, THE PEAK OF HIGHER PERCENTAGE (AND THE RESPECTIVE PERCENTAGE) WAS SHOWN..... 28

TABLE 3 - DLS MEASUREMENTS OF HYDRODYNAMIC DIAMETER (NM) OF 10NM AND 20NM COATED SILVER NANOPARTICLES, 0H AFTER SOLUTIONS PREPARATION (T=0) – 10, 50 AND 100µG/ML. SOLUTIONS WERE PREPARED BY DILUTION WITH COMPLETE GROWTH MEDIA - A-MEM - 10% FBS. IN THE PRESENCE OF MORE THAN ONE PEAK OF SIZE DISTRIBUTION, THE PEAK OF HIGHER PERCENTAGE (AND THE RESPECTIVE PERCENTAGE) WAS SHOWN. 31

TABLE 4 - DLS MEASUREMENTS OF HYDRODYNAMIC DIAMETER (NM) OF 10NM AND 20NM COATED SILVER NANOPARTICLES, 24H AFTER SOLUTIONS PREPARATION (T=24) – 10, 50 AND 100µG/ML. SOLUTIONS WERE PREPARED BY DILUTION WITH COMPLETE GROWTH MEDIA - A-MEM - 10% FBS. IN THE PRESENCE OF MORE THAN ONE PEAK OF SIZE DISTRIBUTION, THE PEAK OF HIGHER PERCENTAGE (AND THE RESPECTIVE PERCENTAGE) WAS SHOWN. 31

TABLE 5 - DLS MEASUREMENTS OF HYDRODYNAMIC DIAMETER (NM) OF 10NM AND 20NM COATED SILVER NANOPARTICLES, 0H AFTER SOLUTIONS PREPARATION (T=0) – 10, 50 AND 100µG/ML. SOLUTIONS WERE PREPARED BY DILUTION WITH COMPLETE GROWTH MEDIA – F-12K - 10% FBS. IN THE PRESENCE OF MORE THAN ONE PEAK OF SIZE DISTRIBUTION, THE PEAK OF HIGHER PERCENTAGE (AND THE RESPECTIVE PERCENTAGE) WAS SHOWN. 32

TABLE 6 - DLS MEASUREMENTS OF HYDRODYNAMIC DIAMETER (NM) OF 10NM AND 20NM COATED SILVER NANOPARTICLES, 24H AFTER SOLUTIONS PREPARATION (T=24) – 10, 50 AND 100µG/ML. SOLUTIONS WERE PREPARED BY DILUTION WITH COMPLETE GROWTH MEDIA – F-12K - 10% FBS. IN THE PRESENCE OF MORE THAN ONE PEAK OF SIZE DISTRIBUTION, THE PEAK OF HIGHER PERCENTAGE (AND THE RESPECTIVE PERCENTAGE) WAS SHOWN. 32

List of Acronymes and Abbreviations

AgNPs – Silver Nanoparticles

Annexin V - aV

DMSO – Dimethyl sulfoxide

DLS – Dynamic light scattering

EPA – Environmental Protection Agency

FBS – Fetal Bovine Serum

FITC – Fluorescein Isothiocyanate

F-12K - Kaighn's Modification of Ham's F-12 Medium

NMs – Nanomaterials

NPs – Nanoparticles

NSCLC - non-small cell lung carcinoma

PBS – Phosphate buffer saline

PI – Propidium iodide

PS – Phosphatidylserine

PVP – Polyvinylpyrrolidone

QDs - Quantum dots

ROS – Reactive Oxygen Species

SCLC - small cell lung carcinoma

Index

List of Figures ..... *i*

List of Tables..... *ii*

List of Acronymes and Abbreviations ..... *iii*

1. Introduction..... *7*

1.1 Historical Overview *10*

1.2 Nanoparticles Description **10**

1.3 Nanoparticles Classification **11**

1.4 Nanoparticles Sources **12**

1.5 Nanoparticles applications **13**

1.6 Nanotoxicology **13**

1.7 Silver Nanoparticles **14**

1.8 Toxicity assessment - Techniques and Biomarkers **16**

1.8.1 Cell proliferation/viability 17

1.8.1.1 MTT Assay 17

1.8.2 Cell cycle analysis 18

1.8.3 Apoptosis/Necrosis 18

1.9 MG-63 cell line **19**

1.10 A549 cell line **20**

1.11 Aims **21**

2. Material and Methods *22*

2.1 Mg-63 osteoblast cell line culture **22**

2.2 A549 Human alveolar adenocarcinoma cell line culture **22**

2.3 Trypsinization **22**

2.4 AgNP Exposure **23**

2.5 Charactertization of AgNPs **23**

2.6 Cell proliferation and cell viability **24**

2.6.1 Trypan Blue Exclusion test 24

2.6.2 MTT Assay 24

2.7 Cell Cycle Analysis – Flow Cytometry **25**

2.8 Apotosis – Annexin V Assay **26**

2.9 Statistical Analysis **27**

3. Results ***28***

3.1 Uncoated and Unstabilized AgNPs **28**

3.1.1 Characterization of AgNPs **28**

3.1.2 Confluence and Morphology **28**

3.1.3 Cell proliferation and Viability **30**

3.1.3.1 Trypan Blue Exclusion Test 30

3.1.3.2 MTT – Assay 30

3.2 PVP Coated AgNPs **31**

3.2.1 Characterization of AgNPs **31**

3.2.2 Confluence and Morphology **32**

3.2.3 Cell Viability – MTT Assay **33**

3.2.4 Cell cycle Analysis – Flow cytometry **37**

3.2.5 Apoptosis –Annexin V Assay **39**

4. Discussion ***41***

5. Conclusion and Future Perspectives ***45***

6. References ***46***

1. Introduction

Publications:

Introduction partially published in an international journal: C. Remédios, **F. Rosário**, and V. Bastos, "Environmental Nanoparticles Interactions with Plants: Morphological, Physiological, and Genotoxic Aspects," Journal of Botany, vol. 2012, Article ID 751686, 8 pages, 2012. doi:10.1155/2012/751686.

Research experiment was partially published in international and national congresses.

Research experiment will be submitted to an international Journal.

1.1 Historical Overview

In 1959, Richard Feynman, an American physicist and Nobel laureate, firstly used the concept of nanotechnology, as a title for one of his articles, reporting a lecture "There's plenty room at the bottom"(Maynard et al., 2006).

The Japanese researcher Professor Norio Taniguchi, in 1974, was the first to define the term nanotechnology, reporting "nanotechnology mainly consists of the processing of separation, consolidation, and deformation of materials by one atom or by one molecule." Later, in 1980, Dr. K. EricDrexler explored the concept of this emerging field, in particular promoting technological significance of nanoscale phenomena and devices. More recently, in 2000, to coordinate federal nanotechnology research and development, the United States National Nanotechnology Initiative was founded (e.g., see http://www.nano.gov/).

Nowadays, nanotechnology is a revolutionary science, with predicted evolution within the next decades that may have equivalence with the ones observed for other industries, as the one of computers during the second half of the last century or earlier with the automobile industry (please see http://www.nanotechnologyresearchfoundation.org/nanohistory.html).

This emerging nanoparticles (NPs) industry is expected to contribute to diverse products and services and to serve multiple consumers' purposes.

However, and despite the success of nanotechnology, the release of NPs to the environment remains unknown, mostly due to the lack of scientific knowledge concerning the potential health and environmental risks associated with nanomaterials (NMs).

Despite this, NPs are being considered in the restrict group of emerging contaminants by, for example, some European countries (e.g., http://files.nanobio-raise.org/Downloads/scenihr.pdf) and the United States Environmental Protection Agency (EPA) (e.g., http://www.epa.gov/fedfac/pdf/emerging_contaminants_nanomaterials.pdf).

1.2 Nanoparticles Description

The unit nanometer was derived from the Greek "nano" which means "dwarf," since nanometers are referred to particles smaller than 1000nm or 1 μm (Buzea et al.,

2007). However, NMs have been considered to be substances with a dimension less than 100nm (Farré et al., 2011; Nowack and Bucheli, 2007; Walker and Bucher, 2009). NPs, considered the building blocks of nanotechnology (Stern and McNeil, 2008), have at least one dimension at 100nm or less, which provides a high surface/volume ratio, leading to high reactivity (increasing the potential to cross cell membranes) (Farré et al., 2011) or intrinsic toxicity of the surface (Das and Ansari, 2009; Donaldson et al., 2004). These factors act together and can change or enhance properties of NPs, such as strength, electrical properties, and optical characteristics (Farré et al., 2011).

1.3 Nanoparticles Classification

The main important thing in nano dimension is that the properties of particles are far different than bulk scale properties and besides, their small size and large surface area can´t determine the harmful potential of NPs (Donaldson et al., 2006). NPs can be classified regarding to their dimensionality, morphology, composition, uniformity, and agglomeration (Buzea et al., 2007), since they can be spherical, tubular, irregularly shaped and can also exist in fused, aggregated or agglomerated forms. Dimensionality refers to their shape or morphology, which can classify them on their number of dimensions, such as one-dimensional (1D), two-dimensional (2D), three-dimensional (3D) NMs (Nowack and Bucheli 2007. The characteristics to be taken relatively to NPs morphology are flatness, sphericity, and aspect ratio. NPs can be composed of single or several materials; composites of various agglomerated materials can be found in nature, although single composites can be easily synthesized today. In respect to uniformity and agglomeration, NPs can exist as dispersed aerosols, suspensions/colloids, or in agglomerate state, due to their different chemistry and electromagnetic properties. Despite some diverse classifications of NPs that can be found, one can in general divide the following classes according to their composition (e.g., (EPA. 2007)):

(1) carbon-based materials (e.g., C60 fullerene), with particular potential in carbon nanotubes technology,

(2) metal-based substances (e.g., Ag, Au, and nanometal oxides), among the last ones, for example, those of titanium oxide are of particular interest,

(3) dendrimers, polymers consisting of branched units,

(4) bio-inorganic complexes (e.g., titanium with attached DNA strands) (EPA. 2007).

1.4 Nanoparticles Sources

NPs can be derived from natural and anthropogenic sources (engineered and unwanted or incidental NPs) (Biswas and Wu, 2005; Liden, 2011; Walker and Bucher, 2009). The natural processes that produce NPs can be photochemical reactions, volcanic eruptions, forest fires, simple erosion, and by plants and animals (shedding of skin and hair) (Buzea et al., 2007). Otherwise, anthropogenic sources refer to the following:

(1) engineered NMs classified as carbon NMs, metal oxide NPs, zero-valence metal NPs, quantum dots (QDs) and dendrimers (Farré et al., 2011),

(2) unwanted or incidental NPs from by-products of simple combustion, food cooking, and chemical manufacturing; welding or refining and smelting; combustion in vehicle and airplane engines; combustion of treated pulverized sewage sludge; and combustion of coal and fuel oil for power generation.

From their multiple conformation, composition, and nature, NPs present multiple functions and almost infinite applications. Nanotechnology has, therefore, gained a place as an emerging science with a recent rise in interest of NPs, mostly due to our increasing ability to synthesize and manipulate such particles.

Thus, nanoscale materials have a variety of uses in different areas, such as electronic, biomedical, pharmaceutical, cosmetic, energy, environmental, catalytic, and material applications (Nowack and Bucheli, 2007), as described below.

1.5 Nanoparticles applications

NMs have diverse applications, which can be summarized as follows (Biswas and Wu, 2005): sunscreens and cosmetics (nanosized titanium dioxide and zinc oxide in sunscreens, nanosized iron oxide in some lipsticks); shampoos and detergents (nanosized alumina); window panes and ceramic tiles (nanostructured titanium oxides); pharmaceutical products; medical implants; food packaging; biosensors and agents for environmental remediation; water treatment technology; composites (mechanical, optical, electrical, and magnetic properties); clays (construction materials); coatings and surfaces; tougher and harder cutting tools; paints; displays (television screens and computer monitors); batteries (growth in portable electronic equipment); fuel additives; carbon nanotube composites; lubricants (nanosized “ball bearings”); magnetic materials; machinable ceramics; and military battle suits. However, and considering the statement that all technology comes with a price, nanotechnology could lead to environmental hazards and adverse health effects (Maynard et al., 2006).

1.6 Nanotoxicology

Primary geogenic NPs may form as aerosols from, for example, sprays of salts and sulfates mostly from the sea, or as sulfate aerosols from volcanic emissions, or even as forest fires (soot and/or polycyclic aromatic hydrocarbons). Moreover, NPs may be anthropogenically introduced in the environment, for example, intentionally to remediate groundwater and contaminated soil (Flahaut, 2010; Klaine et al., 2008), or also unintentionally by several sources, as research and clinical settings and solid or liquid waste streams production facilities (Ray et al., 2009). The biggest risk of release of this material may occur during transportation to good manufacturers and by intentional releases for environmental application (Flahaut, 2010; Ray et al., 2009). The toxicity and degradation of these compounds in the environment cannot be accurately assessed yet because it depends on the NPs type, physicochemical properties, and also the environment media in which partition and the respective conditions. So, this is a field that requires intense research. For example, it is recognized that research needs to be performed in the following fields: (a) detection of NPs in the environment, (b)

measurement of emissions of NPs, (c) life-cycle of NPs in the environment, (d) toxicity of NPs to the environment, and (e) immediate and longer impact on environment (e.g., http://www.nanocap.eu/). The concern of NPs exposure is due to some important issues, as these materials half-lives that may be months to possibly years, the increase on concentration of anthropic substances since NPs are often produced in a large scale, and because this material is expected to be accumulated and transformed by time and local environmental conditions (Flahaut, 2010; Hardman, 2006). The current knowledge about NPs and the challenges of nanotoxicity assessment lead to a lack of effective regulation of NPs use. Some governmental entities, as EPA, have been conducting efforts in order to not only comprehend the properties of NPs and their potential risks for human health and the environment but also to regulate the use, storage, and disposal of these materials to allow a safe and sustainable nanotechnology development. Although there are no specific environmental laws, NPs cut across some existing EPA regulations. For example, several NMs are considered chemical substances under the Toxic Substances Control Act, and pesticides containing nanotechnology products are regulated under the Federal Insecticide, Fungicide, and Rodenticide Act (see http://www.epa.gov/nanoscience/). Still, a recent report from EPA's Office of Inspector General stated that ". . . EPA does not currently have sufficient information or processes to effectively manage the human health and environmental risks of nanomaterials. . ." and that ". . . EPA has the statutory authority to regulate nanomaterials but currently lacks the environmental and human health exposure and toxicological data to do so effectively" (U.S. EPA, 2011). According to this report, some proposed policies have failed, and others that await approval are facing significant barriers to their effectiveness (U.S. EPA, 2011).

1.7 Silver Nanoparticles

Silver Nanoparticles (AgNPs) are one of the promising products in the nanotechnology industry. AgNPs can be synthesized by several physical, chemical and biological methods from metallic silver, and their specific physicochemical properties may differ from those of the bulk substance or from particles of larger size. This effect is mainly attributed to high surface area to volume ratio, which potentially results in high

reactivity. The development of consistent processes for the synthesis of silver nanomaterials is an important aspect of current nanotechnology research.

From the 1300 NP-containing commercial products, that are recently available on the market, at least 300 products (∼25%) contain AgNPs (Rejeski, 2011)). Besides allowing more vigorous reactions due to increase in surface area/volume ratio (leading to high reactivity or intrinsic toxicity of the surface), another advantage is that AgNPs has a great antimicrobial activity, being used in, wound dressings, clothing, laundry detergents, room sprays, food, catheters, surgery instruments and bone cement (Asharani et al., 2009a; Chaloupka et al., 2010).

AgNPs are mostly smaller than 100 nm, and consist of about 20-15,000 silver atoms and the small size enables the passage through biological membranes (Oberdorster et al., 2005). Different shapes and sizes of AgNP, have been shown to bind and react with proteins, be phagocytosed by immune cells, deposited in tissue, or translocate to other parts of the body, leading to a variety of tissue responses (e.g. generation of reactive oxygen species (ROS), inflammation and cell death). Recent studies reported that AgNPs, reduce mitochondrial activity and increase ROS, deplete antioxidant GSH content (Ahamed et al., 2008; AshaRani et al., 2009b; Beer et al., 2012; Biswas and Wu, 2005; Donaldson et al., 2004; Foldbjerg et al., 2011).

Despite of the wide use of AgNPs, there is no data about their concentration, size or form in which they are present in commercially products. Neither on the amount Ag released. Although concentrations of bioavailable free silver ions, in the natural environment in general are too low to lead to toxicity, it is not known until now whether AgNPs present a threat to the environment.

These NPs, showed to have different interactions with several organisms like, bacteria, virus, daphnia, plants and rats (Allen et al., 2010; Remédios et al., 2012; Semmler et al., 2004).

Though, one of the good examples of positive vs negative effects is the extensively use of AgNP as antimicrobial agent against pathogenic bacteria. The abusive use is leading to negative consequences, against the populations of soil microbes that play beneficial roles in the environment, such as promoting plant growth, element cycling, and

degradation of pollutants. The NPs of Ag, showed both toxicity on pathogenic bacteria (e.g., *Escherichia coli* and *Staphylococcus aureus*) and beneficial effects on microbes, as *Pseudomonas putida*, which has bioremediation potential and is a strong root colonizer (Molina et al., 2006; Ramos-Gonzalez et al., 2005).

1.8 Toxicity assessment - Techniques and Biomarkers

The use of AgNPs has increased along the years, and since these NPs are widely used there is few information on the AgNPs interaction with human organs, tissues and cells, regarding the health implications, occupational risks and hazards.

Several in vitro studies have shown that silver NPs can induce toxic effects such as, induction of apoptosis, inflammation, DNA-strand breaks, point mutations, and oxidative DNA adducts, free radical production and membrane damage (Ahamed et al., 2008; AshaRani et al., 2009b; Deng et al., 2010; Foldbjerg et al., 2011; Jun et al., 2011; Lu et al., 2010). However, due to their characteristics, the real toxicity of NPs can be difficult to assess, as there are a number of factors that can interfere, as: the influence of NPs with toxicity assays. The release of silver ions by nanoparticles, particle dissolution, agglomeration, shape, size and type of surface coating are important characteristics that could induce to wrong results over/underestimating the real toxicity of NPs (Bae et al., 2010; El Badawy et al., 2012; Kittler et al., 2010; Liu et al., 2010a; Wijnhoven et al., 2009).

In vitro studies are a fastest, less expensive and less ethically ambiguous way to evaluate the toxicity, of a wide range of compounds. Respecting the principle of 3R's (Reducement, Refinement and Replacement) it is possible to mimic the in vivo or environmental conditions. The control of culture conditions such as, pH, temperature, nutrient and waste concentrations, is crucial to ensure that the toxicity it is from the compound and not because of unstable culturing conditions. Some of the assays mentioned below have been adapted for the use of microplate readers allowing for a rapid throughput (Weyermann et al., 2005).

1.8.1 Cell proliferation/viability

1.8.1.1 MTT Assay

MTT assay described by Mosmann (Mosmann, 1983) has been widely used as a colorimetric approach, based on the activity of mitochondrial dehydrogenase enzymes in cells. This assay made possible to evaluate viable and proliferating cells. Mithocondrial enzymes of viable cells can perform the cleavage of MTT (tetrazolium salt) into a soluble formazan product. The resulting intracellular purple formazan can be solubilized and quantified by spectrophotometry, and the amount of formazan produced is directly proportional to the number of living cells, being widely accepted as a reliable way to examine cell proliferation (Mosmann, 1983; Twentyman and Luscombe, 1987). The number of assay steps has been minimized to such an extent to fulfill the necessity to process large numbers of samples (Mosmann, 1983). The MTT reagent yields low background absorbance values, in the absence of cells and for each cell type the linear relationship between cell number and signal produced is established, thus allowing an accurate quantification of changes in the rate of cell proliferation (Mosmann, 1983). Although, MTT test it is a standard test with low background absorbance, interference of AgNPs on the redout of light absorption for MTT assay has been described (Kroll et al., 2009; Sabatini et al., 2007; Samberg et al., 2010)

1.8.1.2 Trypan Blue

One of the most used criteria's for characterizing viable from dead cells, is the integrity status of the cell membrane, distinguishing cells with damaged or compromised s. Live or dead cells could be assessed for example by the trypan blue (diazo dye) test. This test, is based on the fact that intact cell membranes are impermeable to the dye and, therefore alive cells exclude trypan blue (also called trypan blue exclusion test), while dead cells uptake it, appearing blue under the microscope or when analyzed by the automated cell counter TC10TM (Bio-Rad, Hercules, CA)(Gregori et al., 2001).

1.8.2 Cell cycle analysis

Cell cycle analysis and proliferation kinetics are two major factors in toxicological studies and tumor progression evaluation. Due to its importance, flow cytometry brought the possibility of performing measurements with speed and precision revolutionizing cell biology and cell cycle studies. Cell cycle is the biological phenomenon where undifferentiated cells originate daughter cells with same genetic characteristics. Cell cycle involves interphase and mitosis. There are four distinct phases in a population of proliferating cells: growth and preparation of the chromosomes for replication (G1 phase), synthesis of DNA and duplication of the centrosome (S phase), preparation for mitosis (G2 phase) and mitosis (M phase) (Nunez, 2001). To uphold the normal progression of the cell cycle and the surveillance of genomic integrity, cells have developed a complex network of DNA repair pathways and cell cycle checkpoints. There are cell cycle checkpoints at G1-S, at G2-M, at the exit of mitosis, and an S-phase checkpoint that detects and responds to DNA damage and replication stress. The checkpoints lie in biochemical signaling pathways to sense various types of structural defects in DNA, or in chromosome function, and provoke a versatile cellular response that activates DNA repair and delays cell-cycle progression. These mechanisms evolved to manage inherent errors and genotoxic stress (cellular metabolites or xenobiotics). Hence, when DNA damage is severe, checkpoints purge such potentially hazardous cells by cell death or induce cell-cycle arrest, to essentially offer the time necessary to repair the damage of the DNA before cell division (Koren, 2007; Palou et al., 2010; Soviknes and Glover, 2008).

1.8.3 Apoptosis/Necrosis

Apoptotic and necrotic cell death can be detected by physiological changes that occur in the cell. An apoptotic cell externalizes phosphatidylserine (PS) from the inner to the outer leaflet of the plasma membrane, as a marker of early apoptosis. While a necrotic cell has a damage and inflamed cell membrane that allows the entry of propidium iodide (PI).

Annexin V is a phospholipid-binding protein (aV) that has a high affinity for PS. The aV conjugated to FITC (fluorescein isothiocyanate) binds to PS, staining early-stage apoptotic cells that externalize it and it can be accessed by flow cytometry. Late-stage apoptotic and necrotic cells can be identified by the binding of PI to nuclear DNA. These cells are stained double positive, both for aV+FITC and PI.

1.9 MG-63 cell line

The bone is extensively exposed to NPs, by medical devices, bone cement and bone implants. The major challenge of tissue engineering is to find appropriate materials that could control infection and also allow bone regeneration. In the past years, AgNPs have been used as supplement, acting like an antimicrobial agent on bone implants and bone cement. The most important characteristics of this supplement it is biocompatibility and non-toxicity (Alt et al., 2004; Chaloupka et al., 2010; Zheng et al., 2010).

In this study, we use MG-63 cell line, which is derived from malignant bone tumor (human osteosarcoma). These cells, exhibit characteristics from osteoblastic-like cells including fibroblast morphology, high levels of alkaline phosphatase activity and osteoblast-like regulated synthesis of osteocalcin and collagen type I (Bilbe et al., 1996; Pautke et al., 2004). Although, these cells share osteoblastic features, their chromosomal alterations lead to abnormal molecular and cellular functions, with multiple tryploidy (Di Palma et al., 2003).

MG-63 is a continuous cell line with infinite growth potential, for a long period of time, relatively easy to culture (grows on an adherent monolayer) and has a high rate of proliferation. These characteristics made MG-63 cell line suitable for this type of in vitro tests.(Di Palma et al., 2003).

1.10 A549 cell line

Since the increase in the industrial production of manufactured nanoparticles, the general population may be extremely more exposed to these particles present in the air. Therefore, the most common and important route of exposure to AgNPs is via occupational inhalation, of airborne particles, possible leading to negative pulmonary effects (Oberdorster et al., 2002; Semmler et al., 2004).

Lung cancer remains the most common type of cancer, in men and women worldwide, and the most common cause of cancer mortality (Jaramillo et al., 2008; Zhao et al., 2005). The most common lung cancers are called carcinomas and arise from epithelial cells. Lung carcinomas can be divided in two main types – small cell lung carcinoma (SCLC) and non-small cell lung carcinoma (NSCLC) – according to their size an appearance. NSCLC can also be divided into three main sub-types - adenocarcinoma (40% of lung cancer and the most common type on non-smokers), squamous-cell lung carcinoma, and large-cell lung carcinoma (Vincent et al., 1977; Zhao et al., 2005).

A549 cells derived from human lung adenocarcinoma, and it has been well-characterized and widely used in *in vitro* toxicity tests (Foster et al., 1998; Lieber et al., 1976). These cells, are quite important since they are responsible for the diffusion of some substances, (e.g. water and electrolytes) across the alveoli. When culture in vitro, these cells are grow as an adherent monolayer, and show multilamellar cytoplasmic inclusions bodies, that are typical from type II alveolar epithelial cells of the lung. Furthermore, these cells, synthetize lecithin (act as a surfactant) with high percentage of disaturated fatty acids (Jaramillo et al., 2008; Lieber et al., 1976). Altogether, A549 cells are suitable to serve as an in vitro model of human adenocarcinoma cells (Lieber et al., 1976).

1.11 Aims

The aim of the present dissertation, it was to evaluate the toxic effects of AgNPs on bone and lung cells.

The osteosarcoma cell line MG-63, has rapid growth and retains most osteoblast like characteristics (Clover and Gowen, 1994) was chosen as model of bone. The human alveolar basal epithelial cell line A549, was chosen as model of lung. Being the lung the main portal entry of inhaled NPs and bone extensively exposed to NPs by medical devices, bone cement and bone implants, both are suitable to serve as model for this study.

These cells were exposed to increasing concentrations of, both uncoated and coated NPs (different surface properties), and cell viability, cell cycle and apoptosis were evaluated.

2. Material and Methods

2.1 Mg-63 osteoblast cell line culture

Mg-63 cell line was cultured in 75 cm^2 (Corning®) culture flasks with 10ml of α-MEM – Minimum Essential Medium (Gibco) supplemented with 10% (v/v) Fetal Bovine Serum (FBS) (Gibco), 10000 units ml^{-1} of penicillin-streptomycin (Gibco) and 2.5 µg/ml of Fungizone (Gibco).

The cell line was maintained at controlled humid atmosphere at 37 °C and 5% CO_2. Cells were routinely observed under microscope to check confluence, contaminations and morphology. Before cells reach approximately 80% confluence (% of cell coverage on the surface area of the culture vessel), they were subcultured.

2.2 A549 Human alveolar adenocarcinoma cell line culture

The A549 cell line was cultured in 75 cm^2 (Corning®) culture flasks with 10ml of Kaighn's Modification of Ham's F-12 Medium (F-12K) supplemented with 10% (v/v) Fetal Bovine Serum (FBS) (Gibco), 10000 units $ml^{-1}$of penicillin-streptomycin (Gibco) and 2.5 µg/ml of Fungizone (Gibco).

The cell line was maintained at controlled humid atmosphere at 37 °C and 5% CO_2. Cells were routinely observed under microscope to check confluence, contaminations and morphology. Before cells reach approximately 80% confluence (% of cell coverage on the surface area of the culture vessel), they were subcultured.

2.3 Trypsinization

As both MG-63 and A549 grow as monolayer, in order to subculture cells, a proteolytic enzyme (trypsin) must be added in order to dissociate cells from the surface area of the culture vessel. The standard process for trypsinization for MG-63 and A549 cells is: 1) Observation of cells under microscope to verify confluence, morphology and possible contaminations; 2) Removal of culture medium; 3) Wash cells with sterile phosphate buffer saline (PBS) pH 7.2 (Gibco); 4) Incubation of cell culture with 0.25%

trypsin/1mM EDTA for 5-10 min at 37 °C, until complete detachment and dissociation; 5) Inhibition of trypsin with the complete growth medium (2x the trypsin volume added to cells); 6) Cell resuspension and counting using hemocytometer; 7) After properly identification of the new culture flask, addition of cell suspension to a proportion of 1:9 – cell suspension:complete growth medium.

2.4 AgNP Exposure

1) Silver nanopowder - <100 nm particle size, 99.5% trace metals basis, obtained by Sigma-Aldrich®. The AgNPs are uncoated and not stabilized, according to the manufacture's data. To obtain the stock solution, silver nanopowder was diluted on complete growth media (5% FBS) and sonicated for 1h.

2) Spherical Silver Nanoparticle - well defined sizes particles (10nm and 20nm), coated with PVP (Polyvinylpyrrolidone), obtained by NanoComposix - (BioPure - 1.0 mg/ml). Stock solution was diluted in complete growth media (α-MEM or F12K) to obtain the desired final dilutions and sonicated for 20 minutes.

For both MG-63 and A549 cell lines, the procedure to exposure was mostly the same. Cells were seeded in multiwell plates and incubated for 24h to adhere under the culture conditions described above. After that period, medium was removed and replaced for the same amount of the desired final dilution of indicated AgNPs. The time of exposure was 24h and 48h in the normal culture conditions and then harvested.

2.5 Charactertization of AgNPs

The AgNPs characterization (size distribution of the AgNPs), was performed using Dynamic light scattering (DLS) - Malvern Zetasizer Nano ZS . This is a laser diffraction method, with a multiple scattering technique, to determine the particle size distribution of NPs. The hydrodynamic diameter (effective diameter of a particle in a liquid environment) of the particles was determined in suspension in the cell culture medium.

1) Silver nanopowder – The uncoated nanoparticles were suspended on complete growth media (α-MEM - 5% FBS) and sonicated for 1h to form homogeneous

mixture and the DLS analysis was performed. The following concentrations were analyzed at 0 h and 24h after preparation – 10, 50, 100, 400µg/ml.

2) Spherical Silver Nanoparticle – After preparation of nanoparticles solutions on complete growth media (α-MEM with 10% FBS for MG-63 cell line and F-12K with 10% FBS for A549 cell line) they were sonicated for 20minutes to remove aggregation. According to the product information, the AgNPs had a particle size of 10nm and 20nm. The exposure dilutions analyzed were 10, 50 and 100µg/ml after 0h and 24h preparation

2.6 Cell proliferation and cell viability

2.6.1 Trypan Blue Exclusion test

On this assay, suspended cells (with growth medium - 10^5cells/ml) were seeded at 24 well plates for 24h hours in order to allow adherence, at the same culture conditions. Afterwards, culture medium was replaced for the equivalent amount of AgNPs concentrations – 0, 5, 10, 50, 100, 200, 400µg/ml, diluted in complete growth medium and incubated for 24h and 48h. For each concentration, three replicates were used. Suspended cells (20µl) were transferred to eppendorfs plus 20µl of trypan blue dye (TC10TM, Bio-Rad, Hercules, CA). Cells were incubated for 3 to 5 min and at the end of incubation period, 10µl of the solution (cells and trypan blue) were added to the slide and the viability was counted in the automated cell counter TC10TM (Bio-Rad, Hercules, CA).

2.6.2 MTT Assay

Cell viability (MG-63 and A549) was measured by MTT assay, according to Lévesque et al (Levesque et al., 2008) with some modifications. One hundred µl of suspended cells at the concentration of 10^5cells/ml were seeded in 96 well plates for 24h for adhesion, at normal culture conditions. After 24h, the culture medium was replaced by 100µl of AgNP in growth medium at the following concentrations: 0, 5, 10, 20, 50, 100µg/ml. At the control wells the culture medium was replaced for the same amount of fresh culture medium.

After AgNP exposure (24h and 48h), 50µl of MTT solution (1 mg/ml in PBS pH 7.2) (Sigma Aldrich) was added to each well and incubated for 4h at normal culture conditions. After that, the medium of each well was replaced by 150µl of Dimethyl sulfoxide (DMSO) and left on a shaking plate for formazan crystals solubilization, for two hours at room temperature protected from light. Lastly, the samples absorbance was measured by a microplate reader (BioTek ®– Gen5™ software) at 570 nm with blank correction. Cell viability was calculated using the following equation:

Relative % Viability = A570 Sample/mean A570 Control x 100.

2.7 Cell Cycle Analysis – Flow Cytometry

Cell analysis was performed according to the method described by Bork et al (Bork et al., 2010) with minor modifications.

On this assay, cells were seeded at six well plates for 24h hours in order to allow adherence, at the same culture conditions. Afterwards, culture medium was replaced for the equivalent amount of AgNPs concentrations – 0, 50, 100µg/ml, diluted in complete growth medium (α-MEM or F12K) and incubated for 24h and 48h. For every concentration, tree replicates were used and cells were daily checked under inverted microscope. At the end of each exposure periods, the medium was removed and cells were trypsinized (360µl trypsin-EDTA solution in each well). Trypsin was inhibited with complete growth medium and then cell suspension was transferred to microtubes. Then, the suspension was centrifuged at 300 g during 5 minutes and carefully ressuspended in 1 ml of PBS pH 7.2. Finally, cells were centrifuged once more at same conditions and ressuspended 85% ethanol at 4 ºC for fixation and stored at -20 ^{o}C until further analysis.

To cell cycle analyses, cells were centrifuged at 300 g during 5 minutes, ressuspended in 1 ml PBS pH 7.2 and vortexed for 15 seconds, and finally, filtered through a 55 µm nylon mesh to remove big clusters. Subsequently, 50 µg/ml of propidium iodide (PI) (Fluka, USA) and 50 µg/ml of RNAse were added (Sigma Aldrich, USA) to stain nuclear DNA and remove RNA from the samples, respectively. Samples were incubated for 20 minutes at dark.

Relative fluorescence intensity was measured in a flow cytometer (Beckman Coulter) equipped with an argon laser - 15 mW, 488 nm. The fluorescence peak sample of G0/G1 cells adjusted to channel 200. Acquisitions were made using SYSTEM II software (v. 3.0, Beckman Coulter, USA). For each sample, the number of events reached approximately 5000. Debris and doublets were excluded by the definition of the specific region (Area vs. FL peak height). Cell cycle analysis was then conducted based on the histogram outputs (Oliveira et al., 2006).

2.8 Apotosis – Annexin V Assay

The apoptotic/necrotic cells ratio was measured by flow cytometry using the FITC Annexin V Apoptosis Detection Kit, from BD Pharmingen™ , by double staining with Annexin and PI. The double staining allows the differentiation from early-stage apoptotic cells (Annexin V-FITC positive/PI negative cells), from late-stage apoptotic/necrotic cells (Annexin V-FITC positive/PI positive), and live cells (Annexin V-FITC negative/PI negative).

To perform this assay, 2ml of suspended cells ($1x10^5$cells/ml) were seeded in 6 well plates. Cells were incubated for 24h to allow adherence and then exposed to the same amount of AgNP concentrations - 0, 50, 100µg/ml, diluted in complete growth medium, and incubated for 24h and 48h.

At the end of the exposure time, cells were trypsinized and transferred to 15ml tubes. Afterwards, cells were centrifuged twice in cold PBS and resuspended in "*1x binding buffer"* (Detection Kit from BD Pharmingem™) ($1x10^5$cells/ml). One hundred µl of the sample were incubated in the dark for 10 minutes at room temperature after addition of 5µl annexin V-FITC and 5µl PI and later, 400 µL of *"1x binding buffer"* was added and samples analyzed by flow cytometry. The 488 nm laser was used for excitation and FITC was detected in FL-1 by a 525/30 BP filter while PI was detected in FL-2 by a 575/30 BP filter. Acquisitions were made using SYSTEM II software (v. 3.0, Beckman Coulter, USA). For each sample, 20 000 cells were analyzed and apoptotic (annexin V+, PI−), necrotic (annexin V+, PI+) and live (annexin V−, PI−) cells were expressed as percentages of the 20000 cells.

2.9 Statistical Analysis

For all experiments, at least 3 replicates, and two independent assays were performed. Data analysis was performed in the software SigmaPlot version 11, by one-way ANOVA analysis of variance (One-way ANOVA) (p <0.05), followed by a Holm-Sidak test (p < 0.05) to evaluate the significance of differences in the parameters. When necessary, data were transformed to achieve normality and equality of variances.

3. Results

3.1 Uncoated and Unstabilized AgNPs

3.1.1 Characterization of AgNPs

In order to evaluate the size distributions of the AgNPs in cell culture medium, DLS was used. According to product information, AgNP powder has <100nm and average size of 60nm. DLS measurements were obtained for the exposure concentrations. For both t=0 and t=24h, it is possible to see that at the higher concentration - 400µg/ml the uncoated NPs showed a huge aggregation behavior. For all the obtained measures (t=0 and t=24h), an upper size distribution than 60 nm, was observed (Tables 1 and 2).

Table 1 – DLS measurements of Hydrodynamic diameter of uncoated AgNPs, 0h after solutions preparations (t=0) – 10, 50, 100 and 400µg/ml. Solutions were prepared by dilution with complete growth media - α-MEM - 5% FBS. In the presence of more than one peak of size distribution, the peak of higher percentage (and the respective percentage) was shown.

	Average size (nm)[a]	Hydrodynamic diameter (nm)			
		10µg/ml	50µg/ml	100µg/ml	400µg/ml
Uncoated AgNPs	60 (>%)	230.2(80%)	137.2	106.4	344.9 (81%)

[a] According to the manufacturer Sigma-Aldrich®.

Table 2 - DLS measurements of Hydrodynamic diameter of uncoated AgNPs, 24h after solutions preparations(t=24) – 10, 50, 100 and 400µg/ml. Solutions were prepared by dilution with complete growth media - α-MEM - 5% FBS. In the presence of more than one peak of size distribution, the peak of higher percentage (and the respective percentage) was shown.

	Average size (nm)[a]	Hydrodynamic diameter (nm)			
		10µg/ml	50µg/ml	100µg/ml	400µg/ml
Uncoated AgNPs	60(>%)	84.25 (77%)	108.1	164.5	460.5

[a] According to the manufacturer Sigma-Aldrich®.

3.1.2 Confluence and Morphology

Cells were observed every exposure period, under the inverted microscope (Nikon® Eclipse TS100) (40x or 100x), to check confluence, contaminations and morphology. MG-63 cells had typical fibroblastic morphology and although the number of adherent cells was a bit higher on 50µg/ml, cell confluence was gradually lost at 200 and 400µg/ml (Fig.1- B, C, D).

At the higher concentration (400 ug/ml) (Fig.1- D, Fig. 2 - C), it's possible to see the agglomeration behavior of AgNPs, since their physicochemical properties are difficult to predict and to control.

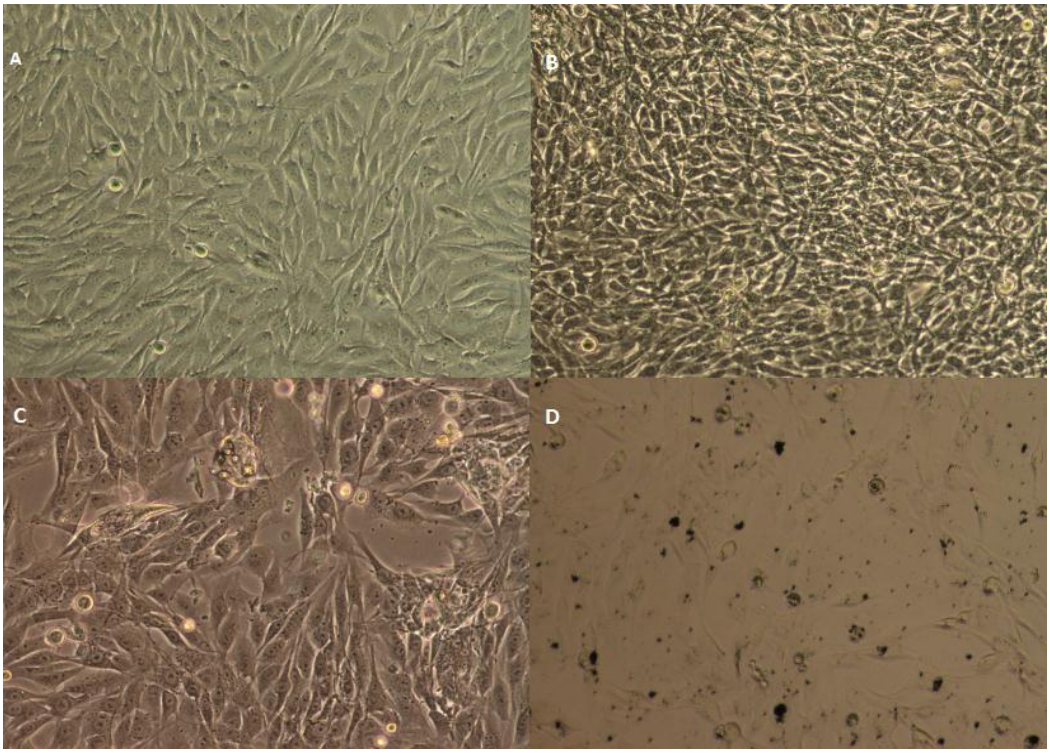

Fig. 1 - Example of MG-63 pictures after 24h of AgNPs exposure: A - Control; B - 50µg/ml; C - 200µg/ml; D - 400µg/ml. 100X.

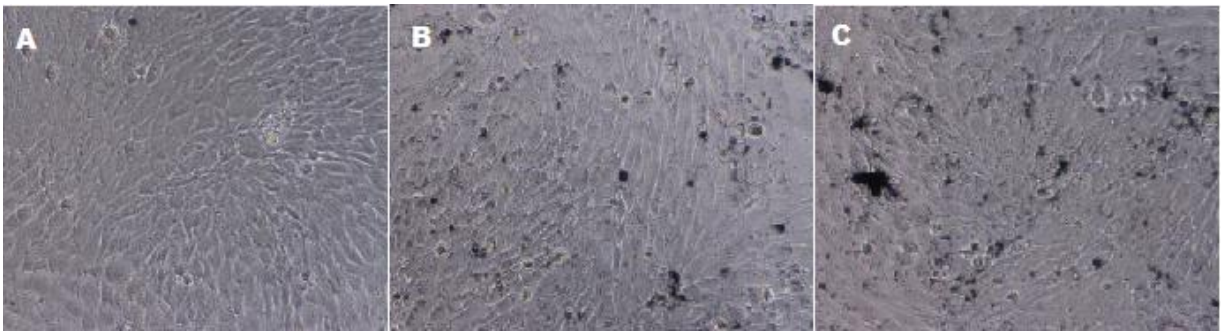

Fig. 2 - Light microscopy images of MG-63 cells exposed to AgNPs for 48h: A - Control; B - 200µg/ml; C - 400µg/ml. 40X

3.1.3 Cell proliferation and Viability

3.1.3.1 Trypan Blue Exclusion Test

Trypan Blue Exclusion Test was used to measure the viability, of MG-63 cell line, based on the exclusion of trypan blue by live cells. Data for 200µg/ml at 48h show a trend to decrease viability despite not significant (P>0.05) (Fig.3). The control values do not show a large variation, as we can see by the small standard deviation, which validates the technique and the test. Unlike the control, all the AgNPs concentrations show a high disparity of results being not possible to make a conclusion on the effects of uncoated AgNPs on MG-63 cell line viability.

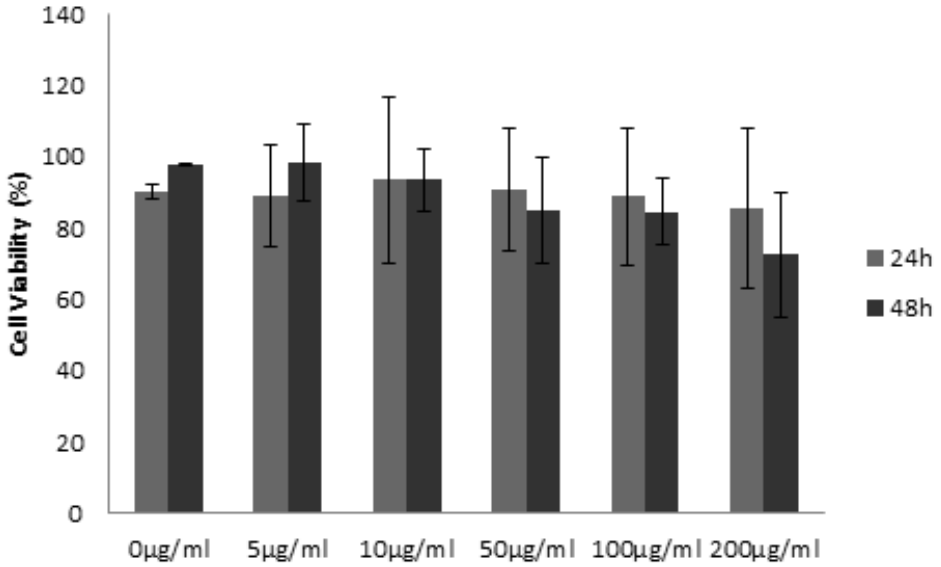

Fig. 3 - Effects of AgNPs on MG-63 cell viability evaluated by two independent Trypan Blue exclusion tests, for 24h and 48h after exposure.

3.1.3.2 MTT – Assay

MTT Assay was used to access the effects of AgNPs on MG-63 cell line viability. As show in Fig.4, there are no significant differences in viability, between AgNP exposed cells and the control for both exposure periods – 24h and 48h. The large standard deviation bars demonstrate the high heterogeneity, and fluctuation of results, before independent exposures leading to inconclusive results.

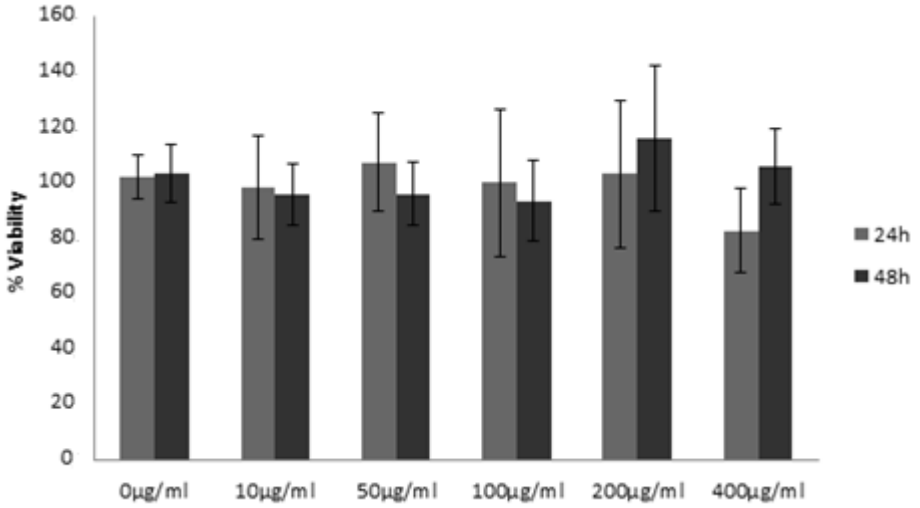

Fig. 4 - Effects of Uncoated AgNPs in MG-63 cell viability (mean ± standard deviation) for 24h and 48h exposure, evaluated by three and two independent MTT assays.

3.2 PVP Coated AgNPs

3.2.1 Characterization of AgNPs

Coated AgNPs were commercially obtained, and their size is defined by 10nm and 20nm. For both α-MEM and F-12K media (for MG-63 and A549 cells, respectively) DLS measurements were performed. AgNPs with 20nm diluted on α-MEM, showed a less tendency to aggregate at t=0 and t=24h (Table 3 and table 4) than 10nm NPs. Also, 10nm AgNPs at the higher concentration showed aggregates, even larger then 100nm (Tables 3 and 4 - 100µg/ml).

Table 3 - DLS measurements of Hydrodynamic diameter (nm) of 10nm and 20nm coated AgNPs, 0h after solutions preparation (t=0) – 10, 50 and 100µg/ml. Solutions were prepared by dilution with complete growth media - α-MEM - 10% FBS. In the presence of more than one peak of size distribution, the peak of higher percentage (and the respective percentage) was shown.

	Average size[a]	Hydrodynamic diameter (nm)		
		10µg/ml	50µg/ml	100µg/ml
AgNPs	10nm	75.66 (62%)	53.02	136.8
AgNPs	20nm	79.77 (83%)	51.04	49.55

[a] According to the manufacturer NanoComposix (Biopure).

Table 4 - DLS measurements of Hydrodynamic diameter (nm) of 10nm and 20nm coated AgNPs, 24h after solutions preparation (t=24) – 10, 50 and 100µg/ml. Solutions were prepared by dilution with complete growth media - α-

MEM - 10% FBS. In the presence of more than one peak of size distribution, the peak of higher percentage (and the respective percentage) was shown.

	Average size[a]	Hydrodynamic diameter (nm)		
		10µg/ml	50µg/ml	100µg/ml
AgNPs	10nm	70.39 (48%)	51.83	378.9
AgNPs	20nm	46.41	44.64	44.93

[a] According to the manufacturer NanoComposix (Biopure).

For F-12K media, it is possible to see that both nanoparticles have a small aggregation behavior even though, also both NPs have larger aggregates than 10nm or 20nm (table 5 and table 6).

Table 5 - DLS measurements of Hydrodynamic diameter (nm) of 10nm and 20nm coated AgNPs, 0h after solutions preparation (t=0) – 10, 50 and 100µg/ml. Solutions were prepared by dilution with complete growth media – F-12K - 10% FBS. In the presence of more than one peak of size distribution, the peak of higher percentage (and the respective percentage) was shown.

	Average size[a]	Hydrodynamic diameter (nm)		
		10µg/ml	50µg/ml	100µg/ml
AgNPs	10nm	49.92 (55%)	75.22 (75%)	81.66
AgNPs	20nm	78.15 (79%)	95.8	52.13

[a] According to the manufacturer NanoComposix (Biopure).

Table 6 - DLS measurements of Hydrodynamic diameter (nm) of 10nm and 20nm coated AgNPs, 24h after solutions preparation (t=24) – 10, 50 and 100µg/ml. Solutions were prepared by dilution with complete growth media – F-12K - 10% FBS. In the presence of more than one peak of size distribution, the peak of higher percentage (and the respective percentage) was shown.

	Average size[a]	Hydrodynamic diameter (nm)		
		10µg/ml	50µg/ml	100µg/ml
AgNPs	10nm	17.19 (77%)	47.85	84.05
AgNPs	20nm	79.78 (78%)	93.93	48.04

[a] According to the manufacturer NanoComposix (Biopure).

3.2.2 Confluence and Morphology

MG-63 and A549 cells were observed every exposure period, under an inverted microscope (Nikon® Eclipse TS100) in a magnification of 40x or 100x, to check confluence, contaminations and morphology. Cell confluence was considerably less at 50µg/ml, for both 10nm and 20nm AgNP exposure (Fig.5 - B, C, D).

At 50µg/ml concentration for the size of 10nm, (Fig.5- B) it's possible to see the agglomeration behavior of AgNPs. A549 cells presented *typical* cuboidal epithelial *aspect*, indicative of type II pulmonary morphology. After 24h exposure to 10nm and 20nm, confluence was less than observed at control (Fig.6 – A, B, C). Despite the visible agglomeration of 10nm AgNP, this treatment shows a higher confluence loss (Fig.6 - B).

No images from 48h after exposure were showed, because there are no visible differences on the images, and the high scatter from AgNPs unable the visibility.

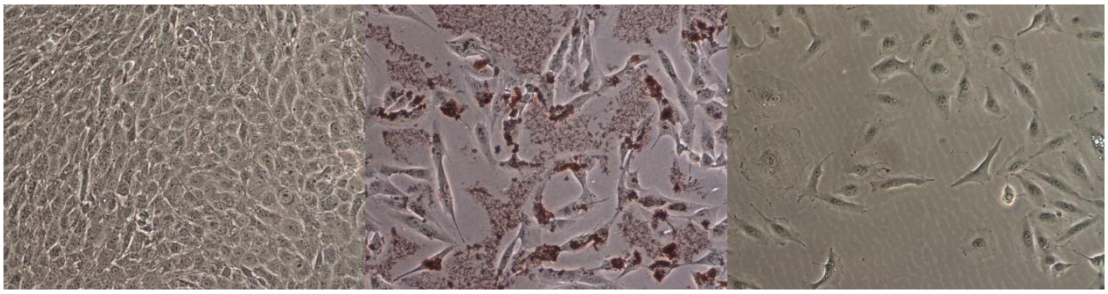

Fig. 5 - Light microscopy images of MG-63 cells exposed to AgNPs for 24h: A - Control; B - 50µg/ml (10nm AgNP); C - 50µg/ml (20nm AgNP). 40X

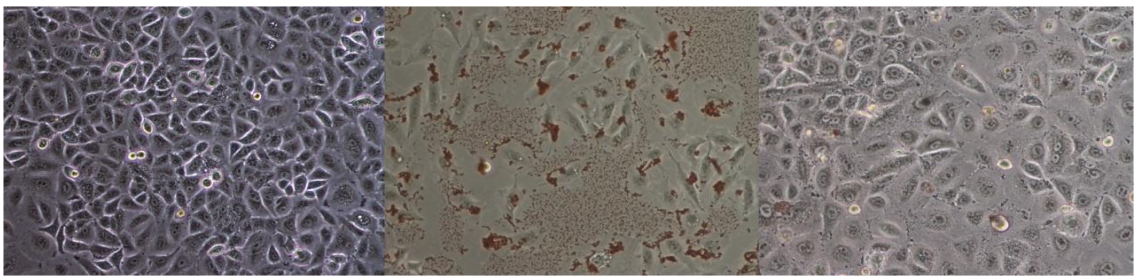

Fig. 6 - Light microscopy images of A549 cells exposed to AgNPs for 24h: A - Control; B - 50µg/ml (10nm AgNP); C - 50µg/ml (20nm AgNP). 40X

3.2.3 Cell Viability – MTT Assay

The MTT Assay was used in order to measure MG-63 and A549 cell lines viability, after 24h and 48h exposure. After 24h of exposure to AgNPs of 10nm and 20nm, a significant decrease on MG-63 cell viability was observed at 50µg/ml for both 10nm and 20nm sizes (Fig.7). For NPs with 10nm, at the higher concentration (100µg/ml), it was possible to see a significant increase on cell viability. In addition, at 100µg/ml significant effects on cell viability were observed between 10nm and 20nm sizes. This test showed

consistent and reliable results based on the small variation of the values, as shown by small standard deviation.

For the 48h exposure (Fig.8), it was possible to see the same pattern of results obtained for 24h. Data shows that at 50µg/ml, a significant decrease on cell viability for 10nm AgNPs and also a significant increase on cell viability for both 10nm and 20 nm AgNPs at 100µg/ml). No significant differences between 10nm and 20nm AgNPs sizes were observed.

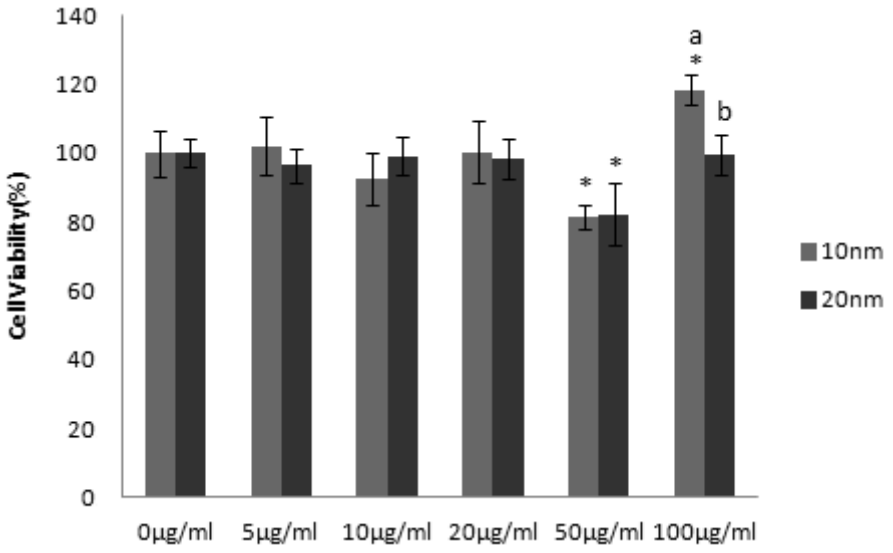

Fig. 7 - Effects of Coated AgNPs – 10nm and 20nm, in MG-63 cell viability (mean ± standard deviation) for 24h exposure, evaluated by three independent MTT assays. Different letters represent differences between AgNPs sizes and * represent differences between concentrations and control.

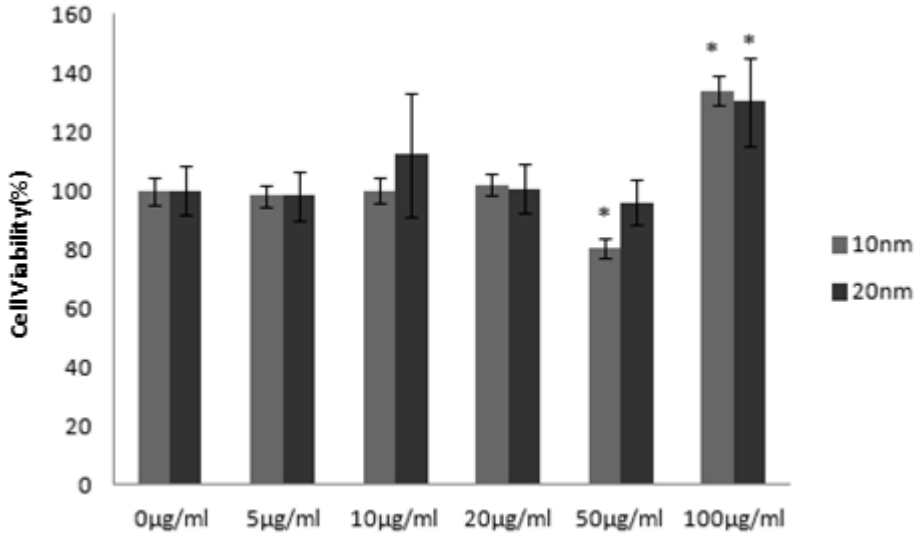

Fig. 8 - AgNPs effects in MG-63 cell viability (%) (mean ± standard deviation) to 48h time of exposure for the MTT Assay. * indicates differences between control and AgNP concentrations ($p < 0.05$).

MTT assay for A549 cell line was performed, also for 24h and 48h exposure, in order to assess the effects of AgNPs on cell viability. Data show that 50µg AgNPs /ml for both sizes (10nm and 20nm) induced for a significant decrease on cell viability after 24h exposure (Fig.9). Although there is no significant difference of cell viability, between control and the higher concentration (100µg/ml), a significant difference between 10nm and 20nm AgNPs sizes response is observed. AgNPs with 10nm show a slightly decrease on cell viability (92%) unlike AgNP with 20nm, that show a stimulation on cell viability (115%).

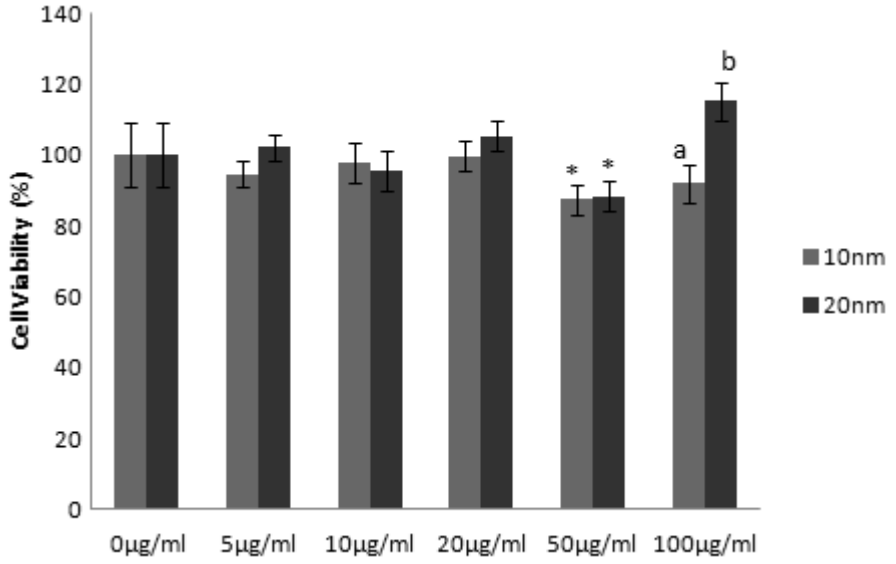

Fig. 9 - Effects of Coated AgNPs – 10nm and 20nm, in A549 cell viability (mean ± SD) for 24h exposure, evaluated by three independent MTT assays. Different letters represent differences between AgNPs sizes within a concentration ($p < 0.05$). * indicates significant differences between AgNPs concentrations and control ($p < 0.05$).

For 48h exposure (Fig.10), 50 µg/ml of AgNPs with 10nm induced at a decreased of 77% on cell viability, while 100µg/ml induced a decrease of 76%. Finally, it is also observed a significant difference within concentrations (50µg/ml and 100µg/ml) between 10nm and 20nm. The 20nm AgNP show a little more propensity to interfere on the redout of MTT assay absorbencies.

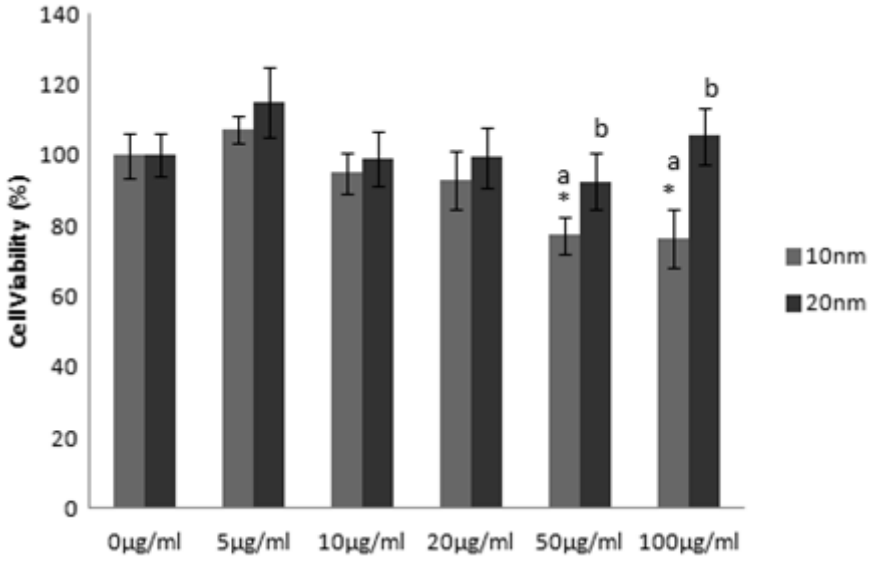

Fig. 10 - AgNPs effects in A549 cell viability (mean ± standard deviation) to 48h time of exposure for the MTT Assay. Different letters within concentrations represent differences between AgNPs sizes ($p < 0.05$). *indicates significant differences between AgNPs concentrations ($p < 0.05$).

In order to measure the interference of AgNPs on the redout of light absorption for MTT assay, as possible explanation for the results obtained for MG-63 and A549 MTT assay at 100µg/ml, an MTT assay for AgNPs (24h) diluted on complete medium but with no cells was performed. As show in Fig.11, after 24h there is a significant increase on absorbance for 50µg/ml and 100µg/ml. As for the 20 nm AgNP, to both 50µg/ml and 100µg/m the absorbance increased 54% and the 145% respectively. Within concentrations, no significant variations were detected between 10nm and 20nm AgNPs.

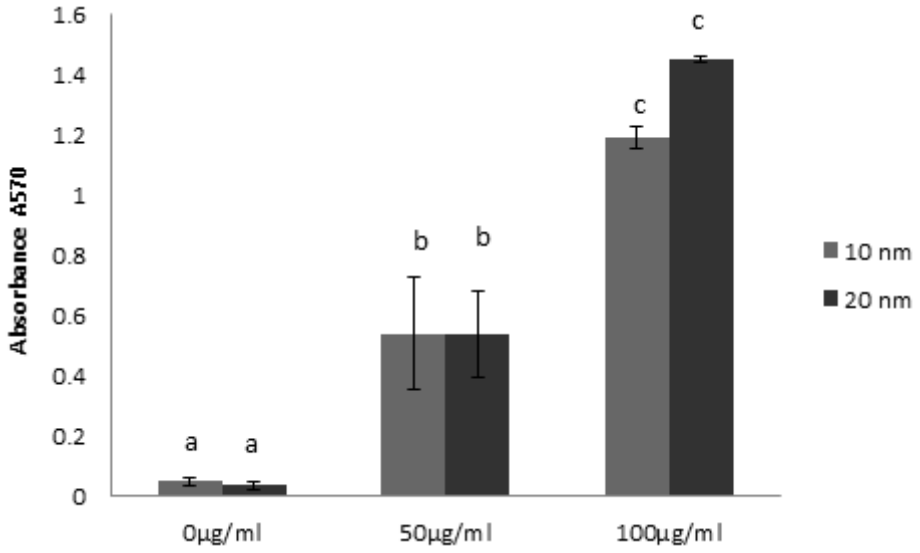

Fig. 11 - Absorbance of MTT assay (mean ± standard deviation) for Coated AgNPs 10nm and 20 nm after 24h, on complete medium with no cells. Different letters represent differences between AgNPs concentrations ($p < 0.05$).

3.2.4 Cell cycle Analysis – Flow cytometry

After 24h exposure, cells (MG-63 and A549) were collected to perform cell cycle analysis and the global cell cycle stages are presented in Figs.12 and 13. In MG-63 cells, for both 10nm and 20nm AgNP there was a significant decrease of Go/G1 cell percentage, with increase in AgNP concentration. For the 100µg/ml concentration, results were significantly different (Fig.12). Also, for both 10nm and 20nm it is possible to see an accumulation of cells on G2 phase.

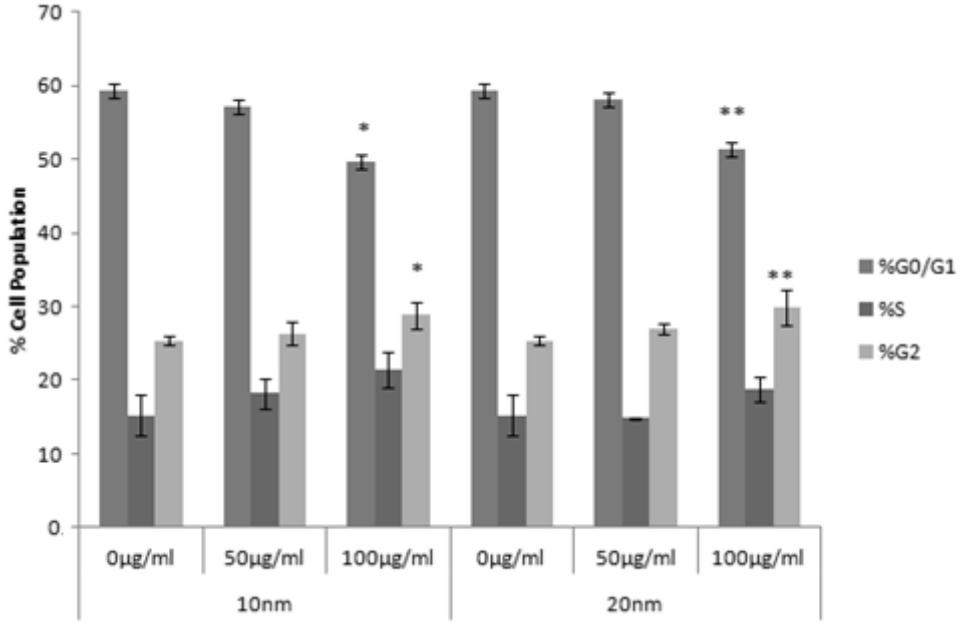

Fig. 12 - Cell cycle results of MG-63 AgNP exposure after 24 h. The given values are the mean % of cell population (± standard deviation) along cell cycle stages of at least 3 replicates. * indicates differences between AgNP size's within a concentration at p <0.05.

For the A549 cell line, the effects of AgNPs on cell cycle were more prominent than for the MG-63 cell line, and large differences were observed. As shown in Fig.13, there is a significant decrease on percentage of G0/G1 cell population and also a significant increase in the percentage of cells in G2 under AgNp exposure, for both 10nm and 20nm.

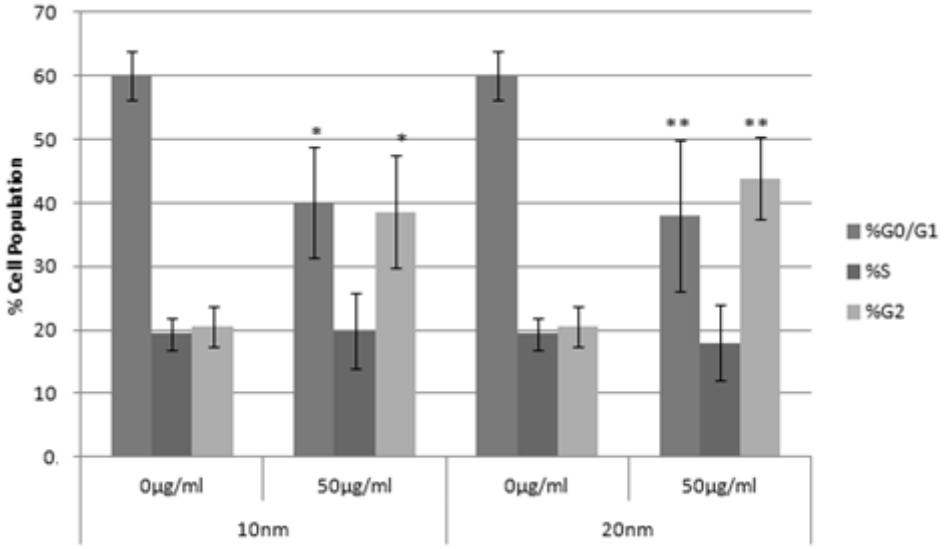

Fig. 13 - Cell cycle results of A549 AgNP exposure after 24 h. The given values are the mean % of cell population (± standard deviation) along cell cycle stages of at least 3 replicates. *indicates differences betwee AgNP size's within a concentration at p <0.05

3.2.5 Apoptosis –Annexin V Assay

Annexin V Assay was used in order to measure the apoptotic/necrotic cells ratio, by flow cytometry using double staining with Annexin V-FITC and PI. The double staining, allows the differentiation from early-stage apoptotic cells, late-stage, apoptotic/necrotic and also from live cells. Both MG-63 and A549 cell lines were exposed, to the concentration of 50µg AgNPs / ml, of both 10nm and 20nm sizes, for 24h and 48h. As show in Figs.14 and 15, there are no significant differences in the percentage of cells under apoptosis for the AgNP concentration of 50µg/ml for both 10nm and 20nm sizes, comparatively to the control in both exposure periods – 24h and 48h.

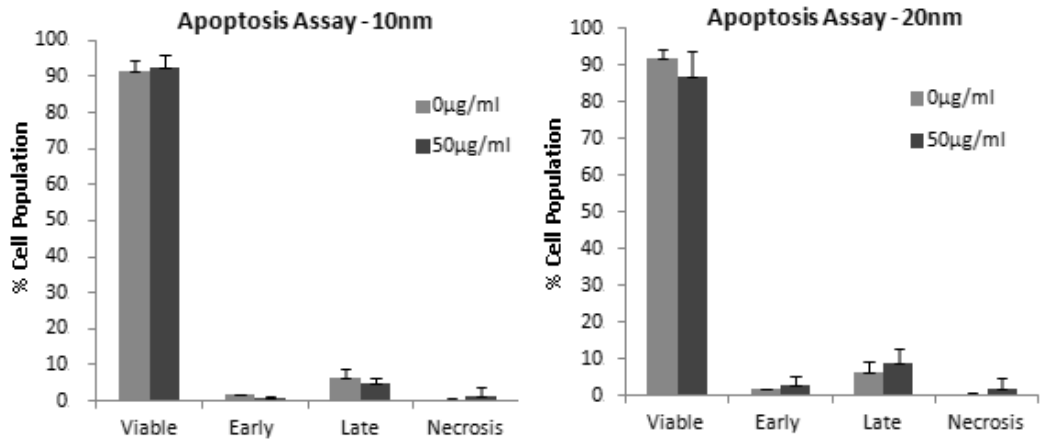

Fig. 14 - Annexin V-FITC assay for apoptosis assessment of MG-63 cell line. Results for 24h exposures to 10nm and 20nm AgNPs with 3 replicates. ± SD.

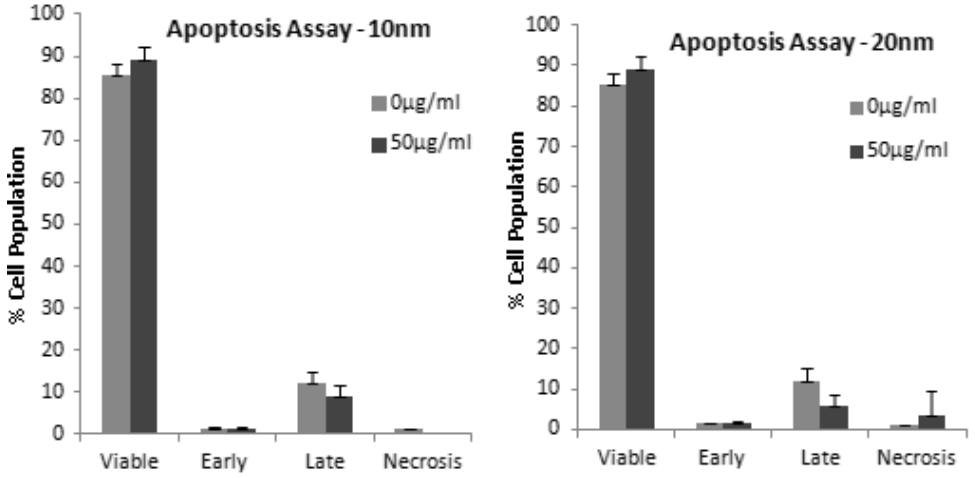

Fig. 15 - Annexin V-FITC assay for apoptosis assessment of MG-63 cell line. Results for 48h exposures to 10nm and 20nm AgNPs with 3 replicates. ± SD. * $p<0.05$.

For A549 cell line (24h exposure), the results (Fig.16) show a significant decrease on the amount of viable cells, for the 10 nm AgNPs in 50µg/ml, and a significant increase on the percentage of late-apoptotic cell (Fig.16 – 10nm). No significant differences were observed, for 24h exposure, between control and 50µg/ml - 20nm AgNPs.

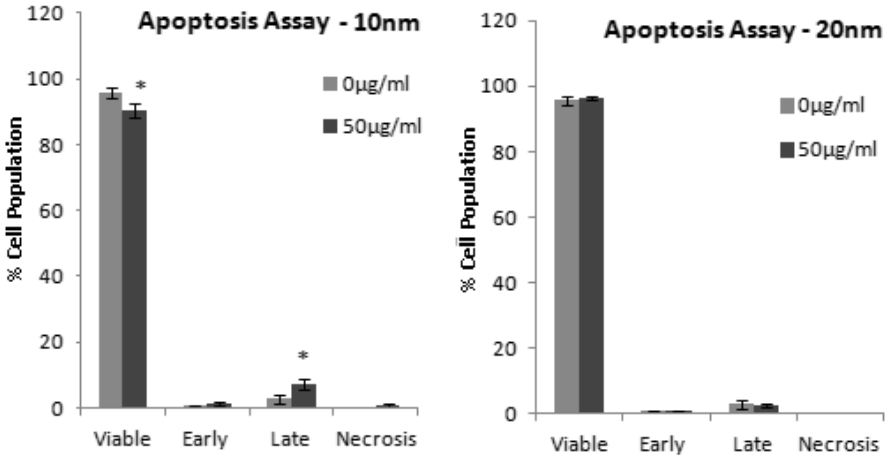

Fig. 16 - Annexin V-FITC assay for apoptosis assessment of A549 cell line. Results for 24h exposure to, 10nm and 20nm AgNPs, with 3 replicates. *indicates differences between control and AgNP concentrations at p <0.05.

The 48 hours assay for A549 cell line, shows at 50 µg/ml, a significant increase the percentage of cells in early and late apoptosis and a decreased the percentage of live cells for both 10nm and 20nm sizes (Fig. 17).

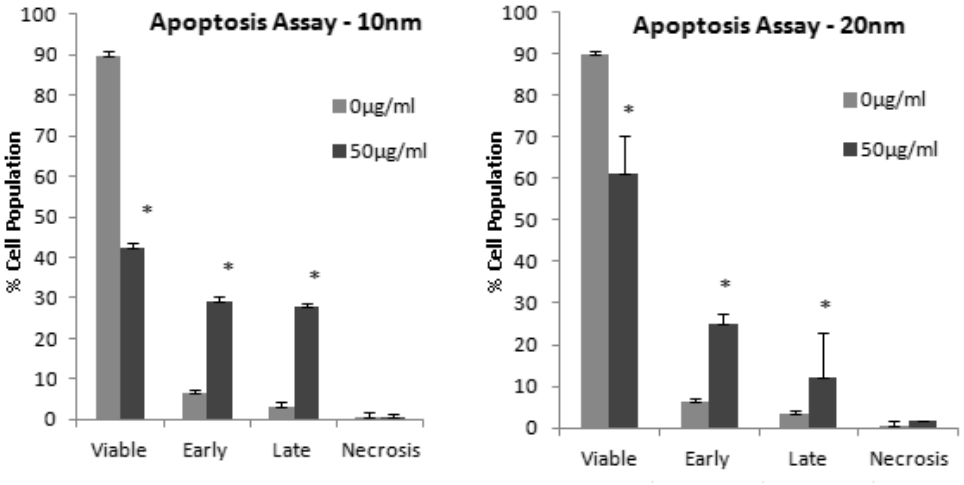

Fig. 17 - Annexin V-FITC assay for apoptosis assessment of A549 cell line. Results for 48h exposure to 10nm and 20nm AgNPs with 3 replicates. * indicates differences between control and AgNP concentrations at p <0.05.

4. Discussion

NPs technology is an emerging field, with multiple potentialities and applications. However, and due to the particular characteristics of NPs, comparatively to their individual components, NPs may present also different toxicity profiles. Despite NPs have always been present in the environment, the concern on their toxicity has only emerged during the last decade. A huge increase of NPs industry, and multiple applications has been noticed *(Donaldson et al., 2006; Lewinski et al., 2008; Medina et al., 2007)*, but the potential for adverse health effects, due to prolonged exposure (through various routes such as skin, respiratory and gastrointestinal tract and blood) at a range of concentration levels, in humans and the environment has not yet been established (Beer et al., 2012; Nagai et al., 2001; Remédios et al., 2012).

The small size/large surface area, and surface properties, are fundamental characteristics of NPs that affect their behavior (adhesion, aggregation, transport, and bioavailability), becoming difficult to predict or asses their toxic effects.

At the first part of this study, uncoated AgNPs with <100nm size (peak size – 60nm) were used. Uncoated AgNPs are more exposed to the surrounding media, and more likely to interact with medium components, leading to higher variations in particles size and stabilization, and this will affect the NPs behavior, being more difficult to predict their effect. (Allen et al., 2010; El Badawy et al., 2012). The used mediums (α-MEM and F-12K) are rich in salts, nutrients and most important, electrolytes and chlorides. These components interfere with, size and stability of NPs, and they may react with silver from the AgNPs and precipitate (silver chloride) or modify the surface charge, so AgNPs may aggregate or even becoming not available at the solution. Furthermore, uncoated metal NPs have typically lyophobic behavior (no affinity for the dispersion medium), and they tend to form large aggregates (that cannot enter the cell), decreasing their bioavailability (Verma et al., 2008). The data obtained on this work, from microscopic observation, and DLS measurements, using uncoated/uncalibrated AgNPs (<100nm), support this facts and it is supported by other authors (Allen et al., 2010; El Badawy et al., 2012; Verma et al., 2008). Both Trypan blue and MTT assay show high heterogeneity and disparity of results,

being impossible to achieve a conclusion. The results obtained by these viability tests, could be explained by the formation of the aggregates. Altogether, assessing as much as possible, the size and chemical speciation of the AgNPs, throughout a particular experiment, with an emphasis on characterization in the media of interest, is imperative.

The evaluation of their toxicological effects, without stabilization and normalization, is complex and leads to inconclusive results being inadequate and particularly burdensome to assess AgNP cytotoxicity *in vitro.*

Coated AgNPs tend to be easier to work with, and less reactive towards surrounding components. These AgNPs, have a great importance, since engineered and manufactured NPs (generally coated) might be released on the environment, at a huge scale, by several sources (Flahaut, 2010; Klaine et al., 2008; Ray et al., 2009; Remédios et al., 2012). Two well defined sizes of AgNPs were used, in order to detect some changes on NPs behavior, and effects on the cellular viability. Both MG-63 and A549 cell's viability data, shows lower standard deviation error than those obtained by uncoated NPs exposure, suggesting more reliable results. Also, for both MG-63 and A549 cell lines it is possible to see a significant decrease in cell viability at the 50µg/ml concentration for the two AgNPs sizes (10nm and 20nm). Other researchers also reported that cell viability was markedly reduced as a function of both culture time and AgNP concentration, in human IMR-90 and U251 cells and in mouse embryonic stem cells (Ahamed et al., 2008; AshaRani et al., 2009b). Although MG-63 data shows a decrease on viability, at the 50µg/ml, an increase on cell viability, at the higher concentration (100µg/ml) is observed for both sizes, especially for 10nm. This increase on cell viability may be justified by the fact that AgNPs aggregation should increase with increasing concentration, reducing the surface area available to which the cells are exposed (El Badawy et al., 2012). DLS results for both AgNPs suspended on α-MEM, for this same concentration (100µg/ml) may explain MTT results, showing that very large aggregates are obtained, especially for the 10nm AgNPs. Another explanation, may relay on the fact that NPs interfere with classic cytotoxicity assays (such as MTT) in a highly concentration-, particle- and assay-specific manner (Kroll et al., 2009; Kroll et al., 2012; Rabolli et al., 2010). Their intrinsic optical absorbance, and adsorption of assay reagents or reporter dyes might interfere with assay components,

resulting in an over/underestimation of their toxicity (Kroll et al., 2012; Rabolli et al., 2010; Sabatini et al., 2007). In particular, we found that AgNPs have a concentration-dependent increase in MTT-formazan light absorption and a concentration-dependent size of aggregates. At the higher concentration - 100µg/ml, as expected, a significant increase on the values of absorbance was observed and may be due to light scattering effect or/and adsorb MTT-formazan crystals, thereby preventing solubilizations. This high absorbance is supported by other authors, and it is conclusive that leads to a false-negative, underestimating AgNPs toxicity (Kroll et al., 2012; Sabatini et al., 2007; Samberg et al., 2010).

In order to examine whether the observed inhibition of cell growth involved changes in the cell cycle phase distribution, the concentrations of 50µg/ml and 100µg/ml, were chosen to assess the effects of AgNPs on MG-63 and A549 cell lines. For the concentration of 50µg/ml a significant decrease on cell viability was observed, while for the concentration of 100µg/ml, a putative false-negative in the MG-63 cell line occurred. At the present work, under the 100µg/ml, MG-63 cell population showed a significant decrease in the percentage of cells at Go/G1, along with concentration increase. Also, with the increase of AgNP dose, the percentage of G_2 population increased. The 100µg/ml concentration showed disturbances on MG-63 cell cycle and also showed a decrease on the number of events counted by flow cytometry. This result helped to validate the hypothesis that a false-negative was obtained on the MTT assay for 100µg/ml - the toxicity for this concentration was underestimated. For the A549 cell line, differences between control and AgNPs concentrations were obtained with lower concentrations (than with MG-63) in the cell cycle data, suggesting that this cell line it is more sensitive. The same trend of response of MG-63 (100µg/ml) was obtained for A549 (50µg/ml), where a decrease in the percentage of cells in Go/G1 and an accumulation in G_2-phase occurred. This result is in agreement with previous findings showing that an increase in the number of cells in G2 phase is related to apoptosis (Lee et al., 2011; Lee et al., 2009; Zhang et al., 2009). When G_2/M checkpoint is activated, cells have chance to repair DNA damages preventing them from entering mitosis or cells may enter in apoptosis.

Additionally, our data indicates that AgNPs also increases cell death by apoptosis, according with the trend to cell cycle arrest at G2 checkpoint. The data from Annexin V assay shown that, already at 24 hours (for A549 cell line), AgNP induced apoptosis. After 24h, exposure to 10nm AgNP induced a decrease on viable cells, and an increase on late apoptotic cells. According to other studies, A549 cells have a constitutively high expression of the heme oxygenase-1, which might render them less susceptible to ROS-induced cell death - early apoptosis (Foldbjerg et al., 2011; Kweon et al., 2006). For 20nm, there were no significant differences between control and 50µg/ml. This may be explained by the fact that exist a size-dependent cellular uptake of SNPs (Liu et al., 2010b). For 48h period, AgNPs (10nm and 20nm) at 50µg/ml, an increase on the number of cells in early and late apoptosis and a decrease in live cell number was found. This increase on apoptotic cells is supported by previous works (Beer et al., 2012; Foldbjerg et al., 2011; Lee et al., 2011; Piao et al., 2011). Although, there is a difference on the type of apoptotic response, – 10nm show higher amount of early apoptotic cells, and 20 nm show a higher amount of late apoptotic cells. A study on DNA fragmentation it is needed to be carried out, since DNA fragmentation is a characteristic from late apoptosis (Foldbjerg et al., 2011). MG-63 cell line showed no differences on live/apoptotic cells, as well as, no significant difference on cell cycle was observed for the same concentration (50µg/ml).

5. Conclusion and Future Perspectives

In conclusion, these results suggest that uncoated/uncalibrated AgNPs lead to inconclusive results, being inadequate and particularly burdensome to assess AgNP cytotoxicity *in vitro.* Although the high reliability of results obtained with coated AgNPs, is still required a careful characterization of particle properties, and an extensive validation of assay systems. Commercial information about NPs is not always the same after they are put in solution and after interaction with surrounding medium. Nps characterization it is a crucial step to understand some of their effects, for both in vitro assays and environmental assessment.

AgNPs can decrease viability of MG-63 and A549 cell line. Higher doses may even interfere on cell cycle, promoting a G_2/M phase arrest along with an increase in apoptosis. A549 cell line appears to be more sensitive to AgNPs than MG-63 cell line, since higher doses are needed for MG-63 to show the same effects.

Therefore, in future work, another trial of cell cycle assay could be performed and DNA damage (comet assay) and oxidative stress (as ROS) should be evaluated in order to understand the pathway that cells go through. Also a validation of assays, especially MTT should be done.

6. References

Ahamed, M., M. Karns, M. Goodson, J. Rowe, S.M. Hussain, J.J. Schlager, and Y. Hong. 2008. DNA damage response to different surface chemistry of silver nanoparticles in mammalian cells. *Toxicology and applied pharmacology*. 233:404-410.

Allen, H.J., C.A. Impellitteri, D.A. Macke, J.L. Heckman, H.C. Poynton, J.M. Lazorchak, S. Govindaswamy, D.L. Roose, and M.N. Nadagouda. 2010. Effects from filtration, capping agents, and presence/absence of food on the toxicity of silver nanoparticles to Daphnia magna. *Environmental toxicology and chemistry / SETAC*. 29:2742-2750.

Alt, V., T. Bechert, P. Steinrucke, M. Wagener, P. Seidel, E. Dingeldein, E. Domann, and R. Schnettler. 2004. An in vitro assessment of the antibacterial properties and cytotoxicity of nanoparticulate silver bone cement. *Biomaterials*. 25:4383-4391.

Asharani, P.V., M.P. Hande, and S. Valiyaveettil. 2009a. Anti-proliferative activity of silver nanoparticles. *BMC cell biology*. 10:65.

AshaRani, P.V., G. Low Kah Mun, M.P. Hande, and S. Valiyaveettil. 2009b. Cytotoxicity and genotoxicity of silver nanoparticles in human cells. *ACS nano*. 3:279-290.

Bae, E., H.J. Park, J. Lee, Y. Kim, J. Yoon, K. Park, K. Choi, and J. Yi. 2010. Bacterial cytotoxicity of the silver nanoparticle related to physicochemical metrics and agglomeration properties. *Environmental toxicology and chemistry / SETAC*. 29:2154-2160.

Beer, C., R. Foldbjerg, Y. Hayashi, D.S. Sutherland, and H. Autrup. 2012. Toxicity of silver nanoparticles - nanoparticle or silver ion? *Toxicology letters*. 208:286-292.

Bilbe, G., E. Roberts, M. Birch, and D.B. Evans. 1996. PCR phenotyping of cytokines, growth factors and their receptors and bone matrix proteins in human osteoblast-like cell lines. *Bone*. 19:437-445.

Biswas, P., and C.Y. Wu. 2005. Nanoparticles and the environment. *J Air Waste Manag Assoc*. 55:708-746.

Bork, U., W.K. Lee, A. Kuchler, T. Dittmar, and F. Thevenod. 2010. Cadmium-induced DNA damage triggers G(2)/M arrest via chk1/2 and cdc2 in p53-deficient kidney proximal tubule cells. *American journal of physiology. Renal physiology*. 298:F255-265.

Buzea, C., Pacheco, II, and K. Robbie. 2007. Nanomaterials and nanoparticles: sources and toxicity. *Biointerphases*. 2:MR17-71.

Chaloupka, K., Y. Malam, and A.M. Seifalian. 2010. Nanosilver as a new generation of nanoproduct in biomedical applications. *Trends in Biotechnology*. 28:580-588.

Clover, J., and M. Gowen. 1994. Are MG-63 and HOS TE85 human osteosarcoma cell lines representative models of the osteoblastic phenotype? *Bone*. 15:585-591.

Das, I., and S.A. Ansari. 2009. Nanomaterials in science and technology. *Journal of Scientific and Industrial Research*. 68:657-667.

Deng, F., P. Olesen, R. Foldbjerg, D.A. Dang, X. Guo, and H. Autrup. 2010. Silver nanoparticles up-regulate Connexin43 expression and increase gap junctional intercellular communication in human lung adenocarcinoma cell line A549. *Nanotoxicology*. 4:186-195.

Di Palma, F., M. Douet, C. Boachon, A. Guignandon, S. Peyroche, B. Forest, C. Alexandre, A. Chamson, and A. Rattner. 2003. Physiological strains induce differentiation in human osteoblasts cultured on orthopaedic biomaterial. *Biomaterials*. 24:3139-3151.

Donaldson, K., R. Aitken, L. Tran, V. Stone, R. Duffin, G. Forrest, and A. Alexander. 2006. Carbon nanotubes: a review of their properties in relation to pulmonary toxicology and workplace safety. *Toxicological sciences : an official journal of the Society of Toxicology*. 92:5-22.

Donaldson, K., V. Stone, C.L. Tran, W. Kreyling, and P.J. Borm. 2004. Nanotoxicology. *Occupational and environmental medicine*. 61:727-728.

El Badawy, A.M., K.G. Scheckel, M. Suidan, and T. Tolaymat. 2012. The impact of stabilization mechanism on the aggregation kinetics of silver nanoparticles. *The Science of the total environment*. 429:325-331.

Farré, M., J. Sanchís, and D. Barceló. 2011. Analysis and assessment of the occurrence, the fate and the behavior of nanomaterials in the environment. *TrAC Trends in Analytical Chemistry*. 30:517-527.

Flahaut, E. 2010. Introduction to the special focus issue: environmental toxicity of nanoparticles. Foreword. *Nanomedicine (Lond)*. 5:949-950.

Foldbjerg, R., D.A. Dang, and H. Autrup. 2011. Cytotoxicity and genotoxicity of silver nanoparticles in the human lung cancer cell line, A549. *Archives of toxicology*. 85:743-750.

Foster, K.A., C.G. Oster, M.M. Mayer, M.L. Avery, and K.L. Audus. 1998. Characterization of the A549 cell line as a type II pulmonary epithelial cell model for drug metabolism. *Experimental cell research*. 243:359-366.

Gregori, G., S. Citterio, A. Ghiani, M. Labra, S. Sgorbati, S. Brown, and M. Denis. 2001. Resolution of viable and membrane-compromised bacteria in freshwater and marine waters based on analytical flow cytometry and nucleic acid double staining. *Applied and environmental microbiology*. 67:4662-4670.

Hardman, R. 2006. A toxicologic review of quantum dots: toxicity depends on physicochemical and environmental factors. *Environmental health perspectives*. 114:165-172.

Jaramillo, M.L., M. Banville, C. Collins, B. Paul-Roc, L. Bourget, and M. O'Connor-McCourt. 2008. Differential sensitivity of A549 non-small lung carcinoma cell responses to epidermal growth factor receptor pathway inhibitors. *Cancer biology & therapy*. 7:557-568.

Jun, E.-A., K.-M. Lim, K. Kim, O.-N. Bae, J.-Y. Noh, K.-H. Chung, and J.-H. Chung. 2011. Silver nanoparticles enhance thrombus formation through increased platelet aggregation and procoagulant activity. *Nanotoxicology*. 5:157-167.

Kittler, S., C. Greulich, J. Diendorf, M. Köller, and M. Epple. 2010. Toxicity of Silver Nanoparticles Increases during Storage Because of Slow Dissolution under Release of Silver Ions. *Chemistry of Materials*. 22:4548-4554.

Klaine, S.J., P.J. Alvarez, G.E. Batley, T.F. Fernandes, R.D. Handy, D.Y. Lyon, S. Mahendra, M.J. McLaughlin, and J.R. Lead. 2008. Nanomaterials in the environment: behavior, fate, bioavailability, and effects. *Environmental toxicology and chemistry / SETAC*. 27:1825-1851.

Koren, A. 2007. The role of the DNA damage checkpoint in regulation of translesion DNA synthesis. *Mutagenesis*. 22:155-160.

Kroll, A., M.H. Pillukat, D. Hahn, and J. Schnekenburger. 2009. Current in vitro methods in nanoparticle risk assessment: limitations and challenges. *Eur J Pharm Biopharm*. 72:370-377.

Kroll, A., M.H. Pillukat, D. Hahn, and J. Schnekenburger. 2012. Interference of engineered nanoparticles with in vitro toxicity assays. *Archives of toxicology*. 86:1123-1136.

Kweon, M.-H., V.M. Adhami, J.-S. Lee, and H. Mukhtar. 2006. Constitutive Overexpression of Nrf2-dependent Heme Oxygenase-1 in A549 Cells Contributes to Resistance to Apoptosis Induced by Epigallocatechin 3-Gallate. *Journal of Biological Chemistry*. 281:33761-33772.

Lee, Y.S., D.W. Kim, Y.H. Lee, J.H. Oh, S. Yoon, M.S. Choi, S.K. Lee, J.W. Kim, K. Lee, and C.W. Song. 2011. Silver nanoparticles induce apoptosis and G2/M arrest via PKCzeta-dependent signaling in A549 lung cells. *Archives of toxicology*. 85:1529-1540.

Lee, Y.S., H.J. Yoon, J.H. Oh, H.J. Park, E.H. Lee, C.W. Song, and S. Yoon. 2009. 1,3-Dinitrobenzene induces apoptosis in TM4 mouse Sertoli cells: Involvement of the c-Jun N-terminal kinase (JNK) MAPK pathway. *Toxicology letters*. 189:145-151.

Levesque, M., C. Martineau, C. Jumarie, and R. Moreau. 2008. Characterization of cadmium uptake and cytotoxicity in human osteoblast-like MG-63 cells. *Toxicology and applied pharmacology*. 231:308-317.

Lewinski, N., V. Colvin, and R. Drezek. 2008. Cytotoxicity of nanoparticles. *Small*. 4:26-49.

Liden, G. 2011. The European commission tries to define nanomaterials. *The Annals of occupational hygiene*. 55:1-5.

Lieber, M., B. Smith, A. Szakal, W. Nelson-Rees, and G. Todaro. 1976. A continuous tumor-cell line from a human lung carcinoma with properties of type II alveolar epithelial cells. *International journal of cancer. Journal international du cancer*. 17:62-70.

Liu, J., D.A. Sonshine, S. Shervani, and R.H. Hurt. 2010a. Controlled release of biologically active silver from nanosilver surfaces. *ACS nano*. 4:6903-6913.

Liu, W., Y. Wu, C. Wang, H.C. Li, T. Wang, C.Y. Liao, L. Cui, Q.F. Zhou, B. Yan, and G.B. Jiang. 2010b. Impact of silver nanoparticles on human cells: effect of particle size. *Nanotoxicology*. 4:319-330.

Lu, W., D. Senapati, S. Wang, O. Tovmachenko, A.K. Singh, H. Yu, and P.C. Ray. 2010. Effect of surface coating on the toxicity of silver nanomaterials on human skin keratinocytes. *Chemical Physics Letters*. 487:92-96.

Maynard, A.D., R.J. Aitken, T. Butz, V. Colvin, K. Donaldson, G. Oberdorster, M.A. Philbert, J. Ryan, A. Seaton, V. Stone, S.S. Tinkle, L. Tran, N.J. Walker, and D.B. Warheit. 2006. Safe handling of nanotechnology. *Nature*. 444:267-269.

Medina, C., M.J. Santos-Martinez, A. Radomski, O.I. Corrigan, and M.W. Radomski. 2007. Nanoparticles: pharmacological and toxicological significance. *Br J Pharmacol*. 150:552-558.

Molina, M.A., J.L. Ramos, and M. Espinosa-Urgel. 2006. A two-partner secretion system is involved in seed and root colonization and iron uptake by Pseudomonas putida KT2440. *Environmental microbiology*. 8:639-647.

Mosmann, T. 1983. Rapid colorimetric assay for cellular growth and survival: application to proliferation and cytotoxicity assays. *Journal of immunological methods*. 65:55-63.

Nagai, Y., T. Chiba, Z. Tang, T. Akahane, T. Kanai, M. Hasegawa, M. Takenaka, and E. Kuramoto. 2001. Fermi surface of nanocrystalline embedded particles in materials: bcc Cu in Fe. *Phys Rev Lett*. 87:176402.

Nowack, B., and T.D. Bucheli. 2007. Occurrence, behavior and effects of nanoparticles in the environment. *Environ Pollut*. 150:5-22.

Nunez, R. 2001. DNA measurement and cell cycle analysis by flow cytometry. *Current issues in molecular biology*. 3:67-70.

Oberdorster, G., A. Maynard, K. Donaldson, V. Castranova, J. Fitzpatrick, K. Ausman, J. Carter, B. Karn, W. Kreyling, D. Lai, S. Olin, N. Monteiro-Riviere, D. Warheit, and H. Yang. 2005. Principles for characterizing the potential human health effects from exposure to nanomaterials: elements of a screening strategy. *Particle and fibre toxicology*. 2:8.

Oberdorster, G., Z. Sharp, V. Atudorei, A. Elder, R. Gelein, A. Lunts, W. Kreyling, and C. Cox. 2002. Extrapulmonary translocation of ultrafine carbon particles following whole-body inhalation exposure of rats. *Journal of toxicology and environmental health. Part A*. 65:1531-1543.

Oliveira, H., J. Loureiro, L. Filipe, C. Santos, J. Ramalho-Santos, M. Sousa, and L. Pereira Mde. 2006. Flow cytometry evaluation of lead and cadmium effects on mouse spermatogenesis. *Reprod Toxicol*. 22:529-535.

Palou, G., R. Palou, A. Guerra-Moreno, A. Duch, A. Travesa, and D.G. Quintana. 2010. Cyclin regulation by the s phase checkpoint. *The Journal of biological chemistry*. 285:26431-26440.

Pautke, C., M. Schieker, T. Tischer, A. Kolk, P. Neth, W. Mutschler, and S. Milz. 2004. Characterization of osteosarcoma cell lines MG-63, Saos-2 and U-2 OS in comparison to human osteoblasts. *Anticancer research*. 24:3743-3748.

Piao, M.J., K.A. Kang, I.K. Lee, H.S. Kim, S. Kim, J.Y. Choi, J. Choi, and J.W. Hyun. 2011. Silver nanoparticles induce oxidative cell damage in human liver cells through inhibition of reduced glutathione and induction of mitochondria-involved apoptosis. *Toxicology letters*. 201:92-100.

Rabolli, V., L.C. Thomassen, C. Princen, D. Napierska, L. Gonzalez, M. Kirsch-Volders, P.H. Hoet, F. Huaux, C.E. Kirschhock, J.A. Martens, and D. Lison. 2010. Influence of size, surface area and microporosity on the in vitro cytotoxic activity of amorphous silica nanoparticles in different cell types. *Nanotoxicology*. 4:307-318.

Ramos-Gonzalez, M.I., M.J. Campos, and J.L. Ramos. 2005. Analysis of Pseudomonas putida KT2440 gene expression in the maize rhizosphere: in vivo [corrected] expression technology capture and identification of root-activated promoters. *Journal of bacteriology*. 187:4033-4041.

Ray, P.C., H. Yu, and P.P. Fu. 2009. Toxicity and environmental risks of nanomaterials: challenges and future needs. *J Environ Sci Health C Environ Carcinog Ecotoxicol Rev*. 27:1-35.

Remédios, C., F. Rosário, and V. Bastos. 2012. Environmental Nanoparticles Interactions with Plants: Morphological, Physiological, and Genotoxic Aspects. *Journal of Botany*. 2012:8.

Sabatini, C.A., R.V. Pereira, and M.H. Gehlen. 2007. Fluorescence modulation of acridine and coumarin dyes by silver nanoparticles. *Journal of fluorescence*. 17:377-382.

Samberg, M.E., S.J. Oldenburg, and N.A. Monteiro-Riviere. 2010. Evaluation of silver nanoparticle toxicity in skin in vivo and keratinocytes in vitro. *Environmental health perspectives*. 118:407-413.

Semmler, M., J. Seitz, F. Erbe, P. Mayer, J. Heyder, G. Oberdörster, and W.G. Kreyling. 2004. Long-Term Clearance Kinetics of Inhaled Ultrafine Insoluble Iridium Particles from the Rat Lung, Including Transient Translocation into Secondary Organs. *Inhalation toxicology*. 16:453-459.

Soviknes, A.M., and J.C. Glover. 2008. Continued growth and cell proliferation into adulthood in the notochord of the appendicularian Oikopleura dioica. *The Biological bulletin*. 214:17-28.

Stern, S.T., and S.E. McNeil. 2008. Nanotechnology safety concerns revisited. *Toxicological sciences : an official journal of the Society of Toxicology*. 101:4-21.

Twentyman, P.R., and M. Luscombe. 1987. A study of some variables in a tetrazolium dye (MTT) based assay for cell growth and chemosensitivity. *British journal of cancer*. 56:279-285.

Verma, A., O. Uzun, Y. Hu, H.S. Han, N. Watson, S. Chen, D.J. Irvine, and F. Stellacci. 2008. Surface-structure-regulated cell-membrane penetration by monolayer-protected nanoparticles. *Nature materials*. 7:588-595.

Vincent, R.G., J.W. Pickren, W.W. Lane, I. Bross, H. Takita, L. Houten, A.C. Gutierrez, and T. Rzepka. 1977. The changing histopathology of lung cancer. A review of 1682 cases. *Cancer*. 39:1647-1655.

Walker, N.J., and J.R. Bucher. 2009. A 21st century paradigm for evaluating the health hazards of nanoscale materials? *Toxicological sciences : an official journal of the Society of Toxicology*. 110:251-254.

Weyermann, J., D. Lochmann, and A. Zimmer. 2005. A practical note on the use of cytotoxicity assays. *International journal of pharmaceutics*. 288:369-376.

Wijnhoven, S.W.P., W.J.G.M. Peijnenburg, C.A. Herberts, W.I. Hagens, A.G. Oomen, E.H.W. Heugens, B. Roszek, J. Bisschops, I. Gosens, D. Van De Meent, S. Dekkers, W.H. De Jong, M. van Zijverden, A.J.A.M. Sips, and R.E. Geertsma. 2009. Nano-silver – a review of

available data and knowledge gaps in human and environmental risk assessment. *Nanotoxicology*. 3:109-138.

Zhang, L., J. Zhang, C. Hu, J. Cao, X. Zhou, Y. Hu, Q. He, and B. Yang. 2009. Efficient activation of p53 pathway in A549 cells exposed to L2, a novel compound targeting p53-MDM2 interaction. *Anti-cancer drugs*. 20:416-424.

Zhao, J., J.E. Kim, E. Reed, and Q.Q. Li. 2005. Molecular mechanism of antitumor activity of taxanes in lung cancer (Review). *International journal of oncology*. 27:247-256.

Zheng, Z., W. Yin, J.N. Zara, W. Li, J. Kwak, R. Mamidi, M. Lee, R.K. Siu, R. Ngo, J. Wang, D. Carpenter, X. Zhang, B. Wu, K. Ting, and C. Soo. 2010. The use of BMP-2 coupled - Nanosilver-PLGA composite grafts to induce bone repair in grossly infected segmental defects. *Biomaterials*. 31:9293-9300.